

FiLoRA: Focus-and-Ignore LoRA for Controllable Feature Reliance

Hyunsuk Chung ^{*1} Caren Han ^{*1} Yerin Choi ^{†2} Seungyeon Ji ^{†23}
 Jinwoo Kim ¹ Eun-Jung Holden ¹ Kyungreem Han ²⁴

Abstract

Multimodal foundation models integrate heterogeneous signals across modalities, yet it remains poorly understood how their predictions depend on specific internal feature groups and whether such reliance can be deliberately controlled. Existing studies of shortcut and spurious behavior largely rely on post hoc analyses or feature removal, offering limited insight into whether reliance can be modulated without altering task semantics. We introduce **FiLoRA (Focus-and-Ignore LoRA)**, an instruction-conditioned, parameter-efficient adaptation framework that enables explicit control over internal feature reliance while keeping the predictive objective fixed. FiLoRA decomposes adaptation into feature group-aligned LoRA modules and applies instruction-conditioned gating, allowing natural language instructions to act as computation-level control signals rather than task redefinitions. Across text-image and audio-visual benchmarks, we show that instruction-conditioned gating induces consistent and causal shifts in internal computation, selectively amplifying or suppressing core and spurious feature groups without modifying the label space or training objective. Further analyses demonstrate that FiLoRA yields improved robustness under spurious feature interventions, revealing a principled mechanism to regulate reliance beyond correlation-driven learning.

^{*}Equal contribution. [†] These authors contributed equally as second authors. ¹University of Melbourne, Melbourne, Australia ²Brain Science Institute, Korea Institute of Science and Technology, Seoul, Republic of Korea ³Department of Computer Science and Engineering, Korea University, Seoul, Republic of Korea ⁴Division of Bio-Medical Science & Technology, University of Science and Technology KIST School, Seoul, Republic of Korea. Correspondence to: Eun-Jung Holden <eunjung.holden@unimelb.edu.au>, Kyungreem Han <khan@kist.re.kr>.

Proceedings of the 42nd International Conference on Machine Learning, Vancouver, Canada. PMLR 267, 2025. Copyright 2025 by the author(s).

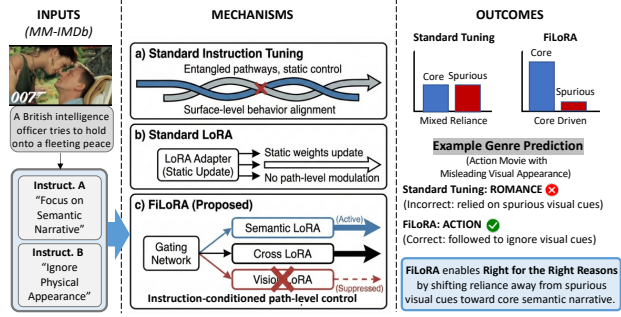


Figure 1. Feature reliance control mechanisms in multimodal models. (a) Standard instruction tuning aligns surface-level behavior without explicitly modulating internal computation. (b) Standard LoRA applies uniform parameter updates without path-level control. (c) FiLoRA (ours) enables instruction-conditioned control by gating feature group-aligned LoRA modules. In a movie genre classification example, FiLoRA suppresses reliance on spurious visual scene cues and grounds predictions in the textual plot, as specified by the instruction.

1. Introduction

Motivated by Feynman’s view “*What I cannot create, I do not understand*”, which suggests that understanding requires the ability to construct and manipulate mechanisms, we ask whether the internal feature reliance of multimodal models can be *explicitly controlled*, rather than merely analyzed post hoc. Recent progress in multimodal foundation models has enabled a single model to process and reason over heterogeneous inputs such as text, vision, and audio (Xu et al., 2025; Google DeepMind, 2025; Ye et al., 2025; Abouelenin et al., 2025). While such models often achieve strong benchmark performance, high accuracy alone provides limited insight into *how* predictions are produced. In many multimodal tasks, correct predictions can be obtained by exploiting superficial or shortcut cues that are correlated with labels in the training distribution, rather than by relying on task-relevant semantic information (Baldassini et al., 2024; Ma et al., 2024; Zhu et al., 2025). For example, movie genre classifiers may rely on visual cues such as poster color or typography that correlate with labels but are not semantically central to the task. This raises concerns about robustness, interpretability, and controllability, especially when deployment conditions differ from training data

(Yang et al., 2023; Agrawal et al., 2018). Existing analysis techniques can retrospectively reveal which features influenced a prediction, but offer no mechanism for explicitly intervening in feature reliance during learning or inference.

Despite increasing awareness of shortcut reliance in multimodal models (Zhang et al., 2024a; Liu et al., 2025; Li et al., 2025; Gao et al., 2025; Zhang et al., 2024c), current learning paradigms lack a principled way to explicitly control which internal feature pathways a model relies on, while keeping the task itself fixed. Instruction tuning affects surface-level outputs without guaranteeing corresponding changes in internal computation (Wu et al., 2024), while full fine-tuning alters feature reliance at the cost of representation drift, entangling reliance shifts with task changes.

This leaves a fundamental question unanswered: *can natural language instructions be used to explicitly control internal feature reliance in multimodal models, without changing the task definition, label space, or base representations?* Recent work has explored using natural language instructions to guide model behavior and feature usage (Zhang et al., 2024b; Stolfo et al., 2025). FIT (Lamb et al., 2025) evaluates whether models follow feature-level guidance expressed in instructions, but assesses control primarily at the level of output behavior and does not provide a mechanism to modulate internal computation pathways. FocalLoRA (Shi et al., 2025) allocates adaptation capacity based on instruction hierarchy, but focuses on aligning behavior rather than selectively activating or suppressing feature-specific computation paths under a fixed task.

The goal of this work is not to improve task accuracy, but to enable controlled and interpretable manipulation of feature reliance in multimodal models. We frame instruction following as a controlled experimental intervention, in which the task and label space remain fixed, while different features are assigned different roles (e.g., core or spurious) through instruction design. We propose **FiLoRA (Focus-and-Ignore LoRA)**, an instruction-conditioned, parameter-efficient adaptation framework that enables explicit control over internal feature reliance in multimodal models. FiLoRA extends LoRA by decomposing adaptation parameters into groups corresponding to distinct functional computation pathways, such as semantic reasoning, visual appearance processing, and acoustic feature extraction. Natural language instructions are encoded and mapped to gate values that modulate the contribution of each LoRA group during the forward pass. By keeping the base model frozen and applying instruction-conditioned gating only to LoRA updates, FiLoRA enables soft, sample-wise intervention on internal computation paths while preserving the original task and representations. Supervision is routed according to instruction-defined feature roles, allowing the model to perform the same task under different reliance conditions.

Our contributions are threefold:

(1) We formalize instruction following as a controlled intervention on feature reliance under fixed task semantics. (2) We propose FiLoRA, a grouped and gated LoRA framework enabling differentiable control over internal computation paths. (3) We demonstrate across multimodal benchmarks that instruction-conditioned reliance modulation yields measurable, robust, and interpretable shifts in feature usage without altering the predictive objective.

2. Related Works

Multimodal Instruction Following. Recent advances in multimodal foundation models (Liu et al., 2024; Dai et al., 2023; Wang et al., 2024; Peng et al., 2023) have further explored instruction-guided multimodal reasoning and controllable vision–language behavior, yet such approaches remain focused on output alignment rather than explicit regulation of internal feature reliance. Related efforts on multimodal attention control or prompting (Chefer et al., 2021; Nguyen et al., 2023) primarily modulate attention weights or input saliency, but do not provide explicit mechanisms to regulate feature-level reliance within internal computation. Instead, they often exploit superficial correlations that are predictive under the training distribution but semantically incidental to the task (Baldassini et al., 2024; Ma et al., 2024; Zhu et al., 2025). This phenomenon aligns with prior analyses of shortcut learning and spurious correlations, which show that models often exploit predictive but semantically irrelevant cues when such shortcuts are available (Geirhos et al., 2020; Yuan et al., 2024; Ye et al., 2024). Such spurious reliance, including poster color in movie genre classification, background patterns in emotion recognition, or speaker identity cues in audio–visual datasets, has been repeatedly observed in benchmarks such as MM-IMDb (Arevalo et al., 2017), CREMA-D (Cao et al., 2014), and RAVDESS (Livingstone & Russo, 2018).

Feature Steering and Bias Mitigation. In the text-only domain, recent work has explored feature steering, representation editing, and controllable generation (Lamb et al., 2025; Zhang et al., 2025; Kong et al., 2024; Hedström et al., 2025; Turner et al., 2024; Zou et al., 2025), demonstrating that certain behaviors can be influenced via latent or activation-level control. FIT (Lamb et al., 2025) steers language models via feature-level instructions, but is limited to textual features and does not generalize to multimodal reliance control. They neither distinguish nor selectively suppress visual or acoustic cues, nor do they provide mechanisms to separate core semantic information from spurious modality-specific correlations.

Existing multimodal bias mitigation methods (Agrawal et al., 2018; Zhang et al., 2024c; Liu et al., 2025) operate primarily at training time and aim to reduce dataset-

level correlations, whereas our setting requires test-time, instruction-conditioned control over feature reliance without retraining. Consequently, they cannot accommodate user-specified directives such as “ignore the background” or “do not use speaker identity” during inference. This lack of controllability limits their applicability in interactive or safety-critical scenarios.

Parameter-efficient fine-tuning methods such as LoRA (Hu et al., 2022), QLoRA (Dettmers et al., 2023), adapters (Houlsby et al., 2019), and FocalLoRA (Shi et al., 2025) enable efficient adaptation of large models but rely on static or pre-defined update pathways. While FocalLoRA allocates adaptation capacity unevenly across model components, these methods do not support instruction-conditioned routing or selective activation of feature-specific computation paths, particularly in multimodal settings. Knowledge editing methods such as ROME and MEMAT enable targeted parameter modifications at test time, but focus on altering factual content or stored knowledge rather than regulating feature reliance under fixed task semantics (Meng et al., 2023; Tamayo et al., 2024).

Gap and Motivation. Taken together, prior work lacks a unified mechanism that translates natural language specifications of feature roles into explicit, instruction-conditioned control over internal multimodal computation paths. This gap motivates our work. We argue that enabling instruction-conditioned selective multimodal reasoning requires a mechanism that translates natural language specifications of feature roles into explicit control over internal computation paths. Rather than redefining tasks or modifying labels, our approach treats instructions as controlled interventions on feature reliance. This perspective directly leads to our proposed framework, which operationalizes feature-level instructions as instruction-conditioned routing over parameter-efficient adaptation pathways.

3. Methodology

3.1. Problem Formulation

We consider a single multimodal prediction task with a fixed label space \mathcal{Y} . Each input sample x_i consists of heterogeneous modalities, such as text, vision, and audio, and is associated with a core label $y_i \in \mathcal{Y}$ defined by the original task objective (e.g., movie genre classification or emotion recognition). Throughout this work, the task definition and label space remain invariant across all experimental conditions. Our goal is not to improve task performance by modifying the prediction objective, but to explicitly control which internal feature pathways the model relies on when solving the same task. To support controlled analysis of feature reliance, we additionally define a spurious proxy label $y_i^{(s)} \in \mathcal{Y}$ for each sample. This proxy label is constructed using only a restricted subset of features, such as shallow visual appearance or low-level acoustic cues. Importantly,

both y_i and $y_i^{(s)}$ belong to the same label space \mathcal{Y} ; the distinction lies solely in the evidence used to generate them. The proxy label is used exclusively as a training-time intervention and is never used as an evaluation target. Details of how spurious proxy labels are constructed for each dataset are provided in Appendix G.

3.2. Instruction as Feature-Role Assignment

Each input is paired with a natural language instruction I_i . Rather than redefining the task, instructions are designed to specify the role that different features should play when producing a prediction. For example, an instruction may emphasize semantic information or explicitly request suppression of visual style cues, while the prediction objective itself remains unchanged.

Instructions are the only control signal provided to the model. Formally, each instruction is encoded into a continuous control representation $\mathbf{z}_i = h_\phi(I_i)$, where $h_\phi(\cdot)$ denotes an instruction encoder. This control signal parameterizes the instruction-conditioned gating function introduced in Section 3.5, determining how strongly different internal feature groups are emphasized or suppressed during prediction. Experimental condition labels used to determine supervision are never exposed as model inputs. This design allows instruction-following to be interpreted as a controlled intervention: the task and label space are fixed, while the role assigned to internal features varies according to instruction semantics.

3.3. Base Model and Parameter-Efficient Adaptation

Let f_θ denote a pretrained multimodal language model with parameters θ . To avoid representation drift and confounding effects introduced by full fine-tuning, all base model parameters are frozen during training. Adaptation is performed using low-rank updates in the spirit of LoRA.

Specifically, for a linear transformation with weight matrix $W \in \mathbb{R}^{d_{\text{out}} \times d_{\text{in}}}$, LoRA introduces an additive low-rank update

$$\Delta W = BA^\top,$$

where $A \in \mathbb{R}^{d_{\text{in}} \times r}$ and $B \in \mathbb{R}^{d_{\text{out}} \times r}$ with $r \ll \min(d_{\text{in}}, d_{\text{out}})$. The adapted transformation is given by $W' = W + \Delta W$. While effective for parameter-efficient adaptation, standard LoRA applies a single undifferentiated update per layer. As a result, it lacks a mechanism for selectively controlling reliance on distinct internal computation pathways, motivating the grouped formulation introduced in the next section. Note that we apply LoRA updates to all linear projections in attention and feed-forward blocks, unless otherwise stated.

3.4. Grouped LoRA for Path-Level Control

To enable fine-grained control over internal computation, we decompose LoRA updates into groups aligned with functional computation paths. Specifically, each adapted trans-

formation is written as

$$W' = W + \sum_{g \in \mathcal{G}} \Delta W_g,$$

where each group-specific update ΔW_g is parameterized as a low-rank adaptation, $\Delta W_g = B_g A_g^\top$, with rank $r \ll \min(d_{\text{in}}, d_{\text{out}})$.

Each group $g \in \mathcal{G}$ corresponds to a semantically meaningful computation pathway, such as semantic text processing, visual appearance encoding, cross-modal interaction and fusion, or acoustic feature extraction. The grouping is determined by the model architecture and remains fixed throughout training. This decomposition allows adaptation to be expressed at the level of computation paths rather than individual layers, providing a structural basis for selectively amplifying or suppressing distinct feature pathways.

3.5. Instruction-Conditioned Gating

To translate instruction semantics into controllable modulation of computation paths, we introduce an instruction-conditioned gating mechanism. Each instruction I_i is encoded into a continuous representation and mapped to a gate vector

$$\mathbf{g}(I_i) = \sigma(h_\phi(I_i)) \in [0, 1]^{|\mathcal{G}|},$$

where $h_\phi(\cdot)$ denotes an instruction encoder followed by a linear projection, and $\sigma(\cdot)$ is an element-wise sigmoid. We note that gates are shared across layers but applied consistently to all group-aligned LoRA updates.

The final adapted transformation is given by

$$W' = W + \sum_{g \in \mathcal{G}} g_g(I_i) \Delta W_g,$$

where each gate $g_g(I_i)$ softly scales the contribution of the corresponding group-specific adaptation ΔW_g . This formulation enables continuous, instruction-dependent intervention at the level of computation paths rather than discrete module selection. Gates depend only on the instruction text and are independent of supervision signals. Because the base model is frozen, changes in model behavior can be attributed to instruction-conditioned reliance modulation rather than representational rewiring or task redefinition.

3.6. Supervision Routing Under Controlled Conditions

Each training sample is associated with an experimental condition that determines which supervision signal is used for optimization. In conditions where core evidence is emphasized or spurious cues are suppressed, the target label is the original task label y_i . In conditions designed to stress reliance on spurious features, the target label is the previously defined spurious proxy label $y_i^{(s)}$. Formally, the target label is selected as:

$$y_i^{\text{target}} = \begin{cases} y_i, & \text{if condition emphasizes core features,} \\ y_i^{(s)}, & \text{if condition emphasizes spurious features} \end{cases}$$

The experimental condition for this selection is never revealed to the model. The model observes only the input modalities and the instruction text, and does not receive any explicit signal indicating which supervision is applied. Hence, any learned shift in feature reliance must emerge from the interaction between instruction-conditioned gating and loss optimization, rather than direct conditioning on the experimental setup. At evaluation time, predictions are assessed with respect to the original task labels y_i .

3.7. Training Objective

The primary optimization objective is a standard classification loss,

$$\mathcal{L}_{\text{cls}}^{(i)} = \text{CE}(f(x_i, I_i), y_i^{\text{target}}),$$

which preserves a single-task learning setup across all conditions. To stabilize instruction-conditioned reliance and prevent degenerate gate behavior, we optionally apply a weak, condition-specific gate regularization term that biases the activation of particular groups under certain conditions. Specifically, we use a linear regularizer of the form

$$\mathcal{L}_{\text{gate}}^{(i)} = \sum_{g \in \mathcal{G}} \alpha_g^{(i)} g_g(I_i),$$

where $\alpha_g^{(i)} \in \{-1, 0, +1\}$ encodes whether the corresponding feature group is encouraged, neutral, or discouraged under the current condition.

The full objective for each sample is given by

$$\mathcal{L}^{(i)} = \mathcal{L}_{\text{cls}}^{(i)} + \lambda \mathcal{L}_{\text{gate}}^{(i)},$$

where λ is chosen to be small so that task performance remains the dominant optimization signal and the regularization acts only as a soft inductive bias rather than a hard constraint. The overall training procedure of FiLoRA is summarized in Algorithm 1 in Appendix H.

3.8. Mechanism Interpretation

Under this formulation, instructions do not impose explicit constraints on output behavior, nor do they redefine the prediction task. Instead, they act as continuous control signals that reshape the optimization landscape by modulating the relative utility of different internal computation paths for minimizing the same objective. Through instruction-conditioned gating, reliance on certain feature groups becomes more or less advantageous during training, leading the model to associate instruction semantics with distinct internal reliance patterns. Importantly, this association is learned without exposing the model to condition labels or alternative task definitions. As a result, instruction-following in FiLoRA manifests not only at the output level, but as systematic and measurable shifts in internal path usage. These shifts can be quantified directly through gate statistics and probed indirectly through robustness and intervention-based evaluations. By holding the task, label space, and base representations fixed, this formulation enables causal analysis

of internal feature reliance modulation rather than post-hoc attribution of observed behavior.

Why Parameter-Level Control. One may ask whether activation steering or routing-based methods could provide similar control. However, such approaches intervene after representations have formed and do not alter the optimization incentives that determine which features are learned and relied upon, often yielding fragile or non-persistent effects. FiLoRA instead intervenes at the parameter level, where feature reliance is established, enabling instruction-conditioned modulation to persist under a fixed task objective. Grouped LoRA constitutes a minimal intervention: it is expressive enough to target semantically meaningful computation paths, yet constrained enough to avoid representation drift. This makes parameter-level grouped adaptation essential for causal and controllable reliance modulation.

3.9. Why This Is Not Multi-Task Learning

At first glance, our training setup may resemble multi-task learning, as different supervision signals are used under different experimental conditions. However, this interpretation is incorrect. In multi-task learning, the model is trained to solve multiple prediction problems associated with different objectives or label spaces. In contrast, our formulation maintains a single task and a fixed label space \mathcal{Y} across all conditions. All predictions in our framework correspond to the same semantic objective, such as genre classification or emotion recognition. The use of a spurious proxy label does not introduce a new task; it provides an alternative supervision signal constructed from restricted evidence within the same task definition. Importantly, the model is never trained to infer or condition on task identity.

Crucially, the experimental conditions that determine which supervision signal is used are not provided to the model. The model observes only the input modalities and the instruction text, and therefore cannot switch between tasks or objectives. Any observed differences in behavior or internal computation must arise from instruction-conditioned reliance modulation rather than task-specific learning. We therefore view our setup as a controlled intervention within a single-task learning framework, where supervision routing is used to induce and analyze shifts in internal feature reliance under fixed predictive semantics.

4. Evaluation Setup

We assess whether instruction-conditioned gating enables controllable and robust modulation of internal feature reliance. Rather than optimizing task performance, we examine whether instructions reliably steer internal computation and induce functional effects. All experiments follow a unified training configuration, with full implementation details provided in Appendix L. Instruction datasets are generated using frozen multimodal foundation models, with 1,000

instructions per dataset; details are provided in Appendix J.

4.1. Dataset Description

We select datasets with identifiable feature groups and fixed task semantics to enable controlled analysis of instruction-conditioned feature reliance; detailed criteria are provided in Appendix K.

We use **Tiny MM-IMDb** to prioritize controllability analysis over task performance. It admits fine-grained, separable feature groups within each modality: textual plots contain semantic and narrative cues, while posters exhibit disentangled visual attributes such as color, layout, and typography. These properties allow selective emphasis or suppression of feature groups via instructions. To verify that observed controllability is not an artifact of scale, we additionally evaluate FiLoRA on larger-capacity backbones.

CREMA-D (Cao et al., 2014) contains emotional expressions from a diverse set of actors with controlled variation across identity-related attributes, supporting identifiable audio-visual feature groups. This structure enables analysis of whether reliance modulation generalizes beyond specific identities while reducing identity-specific shortcuts.

RAVDESS (Livingstone & Russo, 2018) provides spoken and sung emotional speech under a balanced recording setup, yielding systematically controllable acoustic feature groups. Its balanced design minimizes spurious correlations and supports causal analysis of audio-feature reliance.

4.2. Backbone Models

We use dataset-appropriate backbones to avoid modality mismatches. For vision-language experiments on MM-IMDb, we use Qwen2.5-VL (7B, 32B) and Gemma-3n-E4B. For audio-visual experiments on CREMA-D and RAVDESS, we use Qwen2.5-Omni-7B alongside AV-HuBERT (Ren et al., 2023) and AudioCLIP (Guzhov et al., 2022). This setup allows us to assess whether instruction-conditioned reliance modulation generalizes across model scales and architectures with different inductive biases; full details are provided in Appendix A.

4.3. Metrics

We evaluate instruction-conditioned controllability using two complementary metrics. *Gate Modulation Range (GMR)* measures whether internal gates respond systematically to contrasting instructions:

$$GMR_g = \mathbb{E} [|g_g(I^{\text{focus}}) - g_g(I^{\text{ignore}})|].$$

Reliance Sensitivity (RS) measures whether such gate modulation has functional impact on predictions:

$$RS_g = \left\| \frac{\partial \log p(y | x, I)}{\partial g_g} \right\|.$$

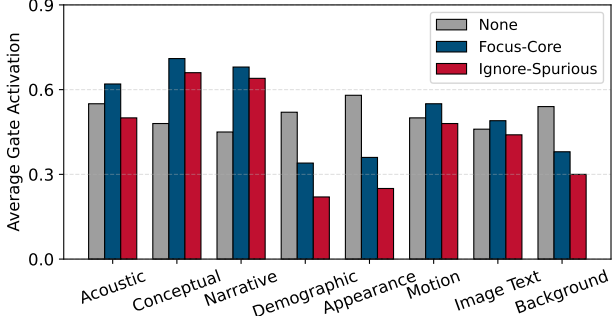


Figure 2. Average gate activations aggregated over taxonomy-aligned feature families under different instruction conditions. Focus-core instructions amplify semantic and narrative features, while ignore-spurious instructions suppress demographic and appearance-related cues, demonstrating structured instruction-conditioned gate control.

Feature Group	MM-IMDb	CREMA-D	RAVDESS
Core	0.42	0.38	0.35
Spurious	0.47	0.41	0.39

Table 1. Gate Modulation Range (GMR) averaged over taxonomy-aligned feature groups (Feature Group). Higher values indicate stronger and more consistent gate responsiveness to instruction changes across datasets.

GMR and RS distinguish superficial gate movement from genuine shifts in feature reliance. In addition, we report decision stability and performance degradation under targeted spurious feature interventions to assess the robustness implications of instruction-conditioned reliance modulation.

5. Results

We organize our results around a sequence of questions that collectively test whether instruction-conditioned gating enables controllable, meaningful, and robust modulation of internal feature reliance.

5.1. Instruction-Conditioned Gate Controllability

We first evaluate whether natural language instructions induce *systematic and semantically aligned* modulation of internal gates, rather than uniform or noisy scaling. Figure 2 visualizes average gate activations aggregated over high-level feature families defined by our feature taxonomy. Rather than exhibiting uniform scaling, different instruction conditions induce distinct and semantically aligned gate configurations. Focus-core instructions amplify gates associated with conceptual and narrative features, while ignore-spurious instructions selectively suppress demographic, appearance, and background features commonly linked to shortcut reliance. Other feature families exhibit moderate or negligible modulation, indicating that instruction-

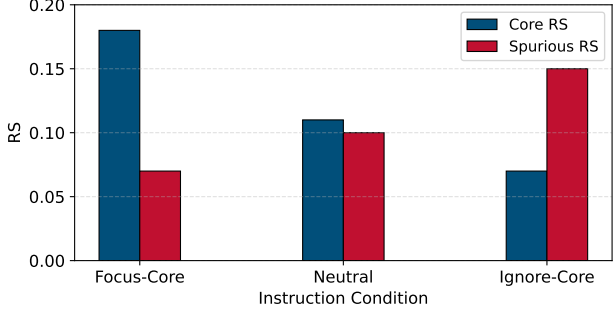


Figure 3. Prediction sensitivity to feature group gate perturbations under different instruction conditions. Reliance Sensitivity (RS) is measured as the average absolute change in the log-probability of the output.

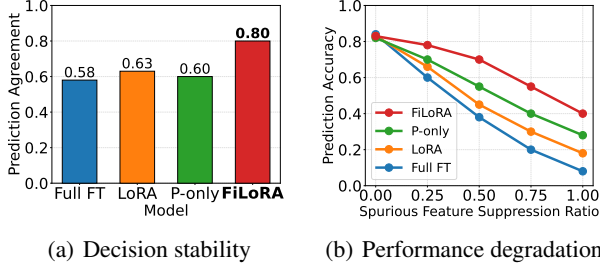
Condition	Core RS	Spurious RS	Core / Spurious ratio
Focus-Core	0.184	0.071	2.59
Neutral	0.112	0.098	1.14
Ignore-Core	0.069	0.153	0.45

Table 2. RS averaged over feature groups. Higher RS indicates a stronger influence of gate perturbations on model predictions.

conditioned gating operates selectively rather than indiscriminately. Table 1 quantifies these trends using Gate Modulation Range (GMR). Across all datasets, both core-associated and spurious-associated feature families exhibit substantial GMR values, demonstrating that instruction-conditioned gating produces consistent and dataset-independent internal modulation. These results establish controllability at the level of structured internal computation paths, showing that instructions consistently modulate feature group-level reliance rather than merely affecting surface behavior or isolated low-level cues. These results should be interpreted in light of the dataset-intrinsic feature composition, which reveals strong modality- and group-level skew in where spurious cues are concentrated (Appendix B), making unregulated reliance particularly prone to shortcut exploitation.

5.2. Functional Impact of Reliance Modulation

We next examine whether instruction-conditioned gate modulation produces functional changes in model behavior. Figure 3 reports prediction sensitivity to feature group gate perturbations, quantified by Reliance Sensitivity (RS). Under focus-core instructions, prediction sensitivity concentrates on core-related feature groups, indicating that the model’s output becomes more dependent on task-relevant signals. Conversely, under instructions that de-emphasize core features, sensitivity shifts toward spurious-related gates. This systematic redistribution of sensitivity demonstrates that gate modulation induces meaningful changes in internal reliance, rather than superficial parameter movement or representation drift.



(a) Decision stability

(b) Performance degradation

Figure 4. Decision stability under spurious feature removal (left) and performance degradation under increasing spurious feature suppression (right). Baselines are evaluated on dataset-appropriate backbones (Qwen2.5-VL for MM-IMDb and Qwen2.5-Omni for CREMA-D/RAVDESS). Full fine-tuning, LoRA, and P-only (prompt-only) baselines exhibit substantial instability and sharp degradation as spurious cues are removed, whereas FiLoRA preserves higher agreement and degrades more gradually, indicating improved robustness through reliance modulation. Full results are shown in Appendix F.

Table 2 quantifies these trends using RS. Under focus-core instructions, core-related feature groups dominate prediction sensitivity, while this relationship reverses under ignore-core instructions. Importantly, RS values under neutral instructions remain balanced, suggesting that the observed shifts are instruction-induced rather than artifacts of the gating architecture. These results confirm that instruction-conditioned gating modulates not only internal activations but also the functional dependency of predictions on specific feature pathways. Together, these results demonstrate that instruction-conditioned gating produces functional and causal changes in model behavior. By selectively reshaping prediction sensitivity, FiLoRA enables controlled reliance shifts that go beyond representational drift or post-hoc attribution. We further verify that this redistribution of reliance sensitivity is consistent across datasets; dataset-wise results are provided in Appendix I.

5.3. Robustness to Spurious Feature Interventions

We next evaluate robustness to spurious feature interventions by examining how model predictions change when spurious cues are disrupted. Rather than measuring raw task performance, we focus on decision stability and degradation behavior, which more directly reflect reliance on shortcut features. For each dataset, all baselines are implemented on the appropriate backbone: Qwen2.5-VL for MM-IMDb and Qwen2.5-Omni for CREMA-D and RAVDESS.

Figure 4(a) reports prediction agreement before and after spurious feature removal across multiple baselines. Full fine-tuning, parameter-efficient adaptation (LoRA), and prompt-only instruction following all exhibit substantial drops in agreement, indicating strong dependence on spurious cues. In contrast, FiLoRA preserves significantly higher decision stability, demonstrating that instruction-conditioned reliance

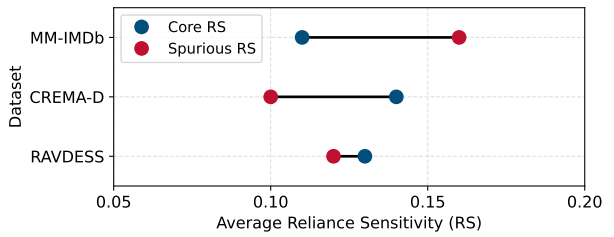


Figure 5. Dataset-wise reliance profiles measured by average RS. Each point reports prediction sensitivity to gate perturbations for core and spurious feature groups under neutral instructions.

modulation effectively reduces sensitivity to spurious feature removal.

To further probe robustness under varying intervention strength, Figure 4(b) shows performance degradation as spurious features are progressively suppressed. Baseline models degrade sharply even under mild suppression, while FiLoRA exhibits a markedly more gradual decline. This difference indicates that FiLoRA reshapes internal reliance structure rather than merely compensating for spurious correlations through additional capacity or prompt conditioning. Together, these results show that robustness emerges from explicit regulation of feature reliance. Unlike full fine-tuning or prompt-based control, FiLoRA enables stable predictions despite substantial spurious feature disruption by dynamically shifting reliance toward core features.

5.4. Dataset-Wise Reliance Profiles

We next analyze how instruction-conditioned reliance modulation manifests across datasets with different intrinsic bias structures. Figure 5 reports the average RS for core and spurious feature groups under focus and ignore instructions. Numerical summaries of these dataset-wise reliance sensitivities are provided in Table 5 in the Appendix.

We observe clear dataset-specific reliance patterns. For MM-IMDb, spurious-related feature groups exhibit higher RS than core groups, reflecting the strong correlation between visual appearance cues and genre labels in movie posters. In contrast, CREMA-D shows substantially higher RS for core feature groups, consistent with emotion recognition being primarily driven by expression-related visual and acoustic signals. RAVDESS lies between these extremes, with comparable RS values for core and spurious groups, indicating a mixed reliance structure. These results demonstrate that FiLoRA does not impose a uniform reliance bias. Instead, it exposes and modulates dataset-intrinsic reliance profiles, enabling controlled analysis of when and where spurious features dominate model behavior. To contextualize these dataset-specific reliance profiles, we analyze which feature groups are most strongly associated with labels. Figure 6 shows the top-20 feature groups ranked by

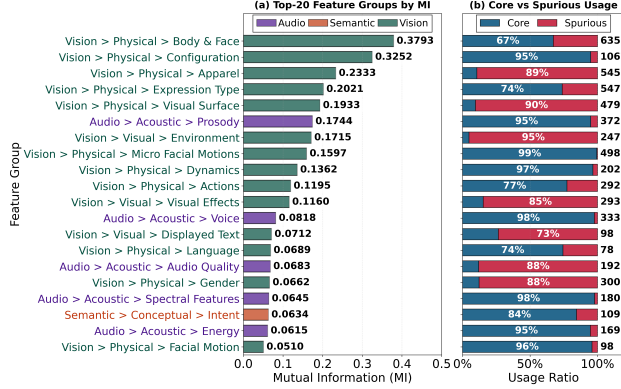


Figure 6. Top-20 feature groups ranked by mutual information with labels. Several highly label-associated features are spurious-dominant, highlighting that correlation-driven learning alone cannot distinguish task-relevant signals from shortcut cues. Full results are provided in Appendix D.

mutual information with labels. Notably, several of the most label-predictive features are spurious-dominant, indicating that strong label association does not necessarily imply task relevance. This dataset-wise variation aligns with our feature–label correlation analysis in Appendix D, which shows that highly label-correlated features are not necessarily core. Importantly, strong label association alone does not imply that a feature is intrinsically more discriminative. As shown in Figure 15 and detailed in Appendix E, label separability measured using spurious-only features is often comparable to that obtained using core-only features across datasets. This indicates that spurious cues can independently support non-trivial label discrimination, explaining why correlation-driven training readily exploits them in the absence of explicit reliance control.

5.5. Generalization Across Model and Scales

We examine the generalization of FiLoRA across model scales and architectures in a dataset-aware manner. Rather than forcing a single backbone family across heterogeneous modalities, we evaluate generalization within the appropriate model class for each dataset to ensure fair and meaningful comparison as shown in Table 3.

MM-IMDb (Vision–Language Models). For MM-IMDb, we evaluate FiLoRA on multiple vision–language backbones, including Qwen2.5-VL-7B, Qwen2.5-VL-32B, and Gemma-VL. Across all VL models, instruction-conditioned gating consistently induces non-trivial GMR and RS. While larger models exhibit higher absolute RS values, the relative ordering between core and spurious feature groups remains stable, indicating that FiLoRA induces scale-invariant control over feature reliance rather than scale-dependent effects.

CREMA-D and RAVDESS (Audio–Visual Models). We evaluate FiLoRA on audio–visual emotion recognition using multiple AV backbones, with Qwen2.5-Omni-7B-Instruct

Dataset	VL / AV Backbone	Core RS	Spurious RS	GMR
MM-IMDb	Qwen2.5-VL-7B	0.11	0.16	0.43
MM-IMDb	Qwen2.5-VL-32B	0.17	0.21	0.51
MM-IMDb	Gemma-3n-E4B	0.10	0.14	0.39
CREMA-D	Qwen2.5-Omni-7B	0.14	0.11	0.45
CREMA-D	AV-HuBERT	0.15	0.10	0.47
CREMA-D	AudioCLIP	0.14	0.11	0.46
RAVDESS	Qwen2.5-Omni-7B	0.13	0.12	0.44
RAVDESS	AV-HuBERT	0.13	0.11	0.43
RAVDESS	AudioCLIP	0.12	0.11	0.42

Table 3. Generalization of FiLoRA across model scales and architectures. We report core and spurious RS and the resulting GMR across vision–language backbones on MM-IMDb and audio–visual backbones on CREMA-D and RAVDESS, demonstrating consistent instruction-conditioned reliance behavior across heterogeneous models.

included as a strong baseline alongside non-Omni architectures. Specifically, we consider audio-centric (AV-HuBERT) and contrastive multimodal (AudioCLIP) models to assess whether reliance modulation persists across different fusion strategies and representational biases. FiLoRA exhibits consistent instruction-conditioned controllability and reliance modulation across all evaluated AV backbones on both CREMA-D and RAVDESS. While absolute RS values vary slightly across architectures, the relative balance between core and spurious feature groups remains stable within each dataset. This consistency across Omni and non-Omni models suggests that FiLoRA does not exploit architecture-specific shortcuts, but instead operates at the level of feature group reliance shared across AV backbones.

Together, these results indicate that FiLoRA does not rely on a specific multimodal architecture. Instead, instruction-conditioned reliance modulation generalizes across VL and AV backbones with fundamentally different inductive biases, demonstrating a backbone-agnostic mechanism for controlling feature reliance.

6. Conclusion

We show that spurious features in multimodal datasets are structurally embedded and often sufficiently predictive to be exploited by correlation-driven learning, explaining why prompt-level control alone is insufficient to regulate internal reliance. We introduce FiLoRA, a lightweight framework for instruction-conditioned reliance steering that modulates internal computation paths without altering inputs or task semantics. Across vision–language and audio–visual settings, FiLoRA improves decision stability under spurious interventions and degrades more gracefully than fine-tuning, LoRA, and prompt-only baselines, demonstrating functional control over internal feature reliance. Overall, our results suggest a reframing of multimodal instruction following: beyond controlling what models predict, it is crucial to control how they use information.

Impact Statement

This work studies how multimodal models rely on different internal features under natural language instructions, and proposes FiLoRA as a mechanism for instruction-conditioned regulation of such reliance. By enabling models to reduce dependence on spurious features while preserving task semantics, this research has the potential to improve the robustness, reliability, and interpretability of multimodal systems deployed in real-world settings, including multimedia analysis, affect recognition, and human-centered AI applications.

At the same time, mechanisms that allow fine-grained control over internal feature usage may introduce new risks if misused. In particular, instruction-conditioned reliance steering could be exploited to intentionally amplify certain biases or suppress relevant information in downstream decision-making systems. Such risks highlight the importance of careful deployment and transparent evaluation when applying reliance-control mechanisms in high-stakes or sensitive domains.

We mitigate these concerns through several design choices. FiLoRA does not alter model inputs or task objectives, and all evaluations are conducted exclusively with respect to the original ground-truth labels. Spurious proxy labels are used only as a training-time diagnostic tool to induce controlled reliance shifts and are never exposed at inference time. Furthermore, our analyses focus on understanding and measuring internal behavior rather than optimizing for performance gains alone.

Overall, we view FiLoRA as a step toward more accountable multimodal modeling, where instruction following is coupled with explicit understanding and regulation of how information is used. We hope this work encourages further research on controllable, interpretable, and responsible internal mechanisms for large multimodal models.

References

Abouelenin, A., Ashfaq, A., Atkinson, A., Awadalla, H., Bach, N., Bao, J., Benhaim, A., Cai, M., Chaudhary, V., Chen, C., et al. Phi-4-mini technical report: Compact yet powerful multimodal language models via mixture-of-loras. *CoRR*, 2025.

Agrawal, A., Batra, D., Parikh, D., and Kembhavi, A. Don't just assume; look and answer: Overcoming priors for visual question answering. In *Proceedings of the IEEE conference on computer vision and pattern recognition*, pp. 4971–4980, 2018.

Arevalo, J., Solorio, T., y Gómez, M. M., and González, F. A. Gated multimodal units for information fusion, 2017.

Baldassini, F. B., Shukor, M., Cord, M., Soulier, L., and Piwowarski, B. What makes multimodal in-context learning work? In *Proceedings of the IEEE/CVF Conference on Computer Vision and Pattern Recognition*, pp. 1539–1550, 2024.

Cao, H., Cooper, D. G., Keutmann, M. K., Gur, R. C., Nenkova, A., and Verma, R. Crema-d: Crowd-sourced emotional multimodal actors dataset. *IEEE Transactions on Affective Computing*, 5(4):377–390, 2014.

Chefer, H., Gur, S., and Wolf, L. Transformer interpretability beyond attention visualization, 2021.

Dai, W., Li, J., Li, D., Tiong, A., Zhao, J., Wang, W., Li, B., Fung, P. N., and Hoi, S. Instructblip: Towards general-purpose vision-language models with instruction tuning. *Advances in neural information processing systems*, 36: 49250–49267, 2023.

Dettmers, T., Pagnoni, A., Holtzman, A., and Zettlemoyer, L. Qlora: Efficient finetuning of quantized llms. *Advances in neural information processing systems*, 36:10088–10115, 2023.

Gao, X., Cao, B., Zhu, P., Wang, N., and Hu, Q. Asymmetric reinforcing against multi-modal representation bias. *AAAI'25/IAAI'25/EAAI'25*. AAAI Press, 2025.

Geirhos, R., Jacobsen, J.-H., Michaelis, C., Zemel, R., Brendel, W., Bethge, M., and Wichmann, F. A. Shortcut learning in deep neural networks. *Nature Machine Intelligence*, 2(11):665–673, November 2020.

Google DeepMind. Gemma 3n model card, 2025.

Guzhov, A., Raue, F., Hees, J., and Dengel, A. Audioclip: Extending clip to image, text and audio. In *ICASSP 2022 - 2022 IEEE International Conference on Acoustics, Speech and Signal Processing (ICASSP)*, pp. 976–980, 2022.

Hedström, A., I. Amoukou, S., Bewley, T., Mishra, S., and Veloso, M. To steer or not to steer? Mechanistic error reduction with abstention for language models. In Singh, A., Fazel, M., Hsu, D., Lacoste-Julien, S., Berkenkamp, F., Maharaj, T., Wagstaff, K., and Zhu, J. (eds.), *Proceedings of the 42nd International Conference on Machine Learning*, volume 267 of *Proceedings of Machine Learning Research*, pp. 22924–22945. PMLR, 13–19 Jul 2025.

Houlsby, N., Giurgiu, A., Jastrzebski, S., Morrone, B., De Laroussilhe, Q., Gesmundo, A., Attariyan, M., and Gelly, S. Parameter-efficient transfer learning for nlp. In *International conference on machine learning*, pp. 2790–2799. PMLR, 2019.

Hu, E. J., Shen, Y., Wallis, P., Allen-Zhu, Z., Li, Y., Wang, S., Wang, L., Chen, W., et al. Lora: Low-rank adaptation of large language models. *ICLR*, 1(2):3, 2022.

Kong, L., Wang, H., Mu, W., Du, Y., Zhuang, Y., Zhou, Y., Song, Y., Zhang, R., Wang, K., and Zhang, C. Aligning large language models with representation editing: A control perspective. In Globerson, A., Mackey, L., Belgrave, D., Fan, A., Paquet, U., Tomczak, J., and Zhang, C. (eds.), *Advances in Neural Information Processing Systems*, volume 37, pp. 37356–37384. Curran Associates, Inc., 2024.

Lamb, T. A., Davies, A., Paren, A., Torr, P., and Pinto, F. Focus on this, not that! steering LLMs with adaptive feature specification. In *ICML 2025 Workshop on Reliable and Responsible Foundation Models*, 2025.

Li, Z., Wen, X., Lou, J., Ji, Y., Lu, Y., Han, X., Zhang, D., and Sun, L. The devil is in the details: Tackling unimodal spurious correlations for generalizable multimodal reward models. In *Forty-second International Conference on Machine Learning*, 2025.

Liu, H., Li, C., Li, Y., Li, B., Zhang, Y., Shen, S., and Lee, Y. J. Llava-next: Improved reasoning, ocr, and world knowledge, January 2024. URL <https://llava-vl.github.io/blog/2024-01-30-llava-next/>.

Liu, Y., Zhu, J., Wen, C., Lu, G., Lin, H., and Chen, B. Towards robust visual question answering via prompt-driven geometric harmonization. In *Proceedings of the Thirty-Ninth AAAI Conference on Artificial Intelligence and Thirty-Seventh Conference on Innovative Applications of Artificial Intelligence and Fifteenth Symposium on Educational Advances in Artificial Intelligence*. AAAI Press, 2025.

Livingstone, S. R. and Russo, F. A. The ryerson audio-visual database of emotional speech and song (ravdess): A dynamic, multimodal set of facial and vocal expressions in north american english. *PLoS one*, 13(5):e0196391, 2018.

Ma, J., Hu, M., Wang, P., Sun, W., Song, L., Pei, H., Liu, J., and Du, Y. Look, listen, and answer: overcoming biases for audio-visual question answering. *NIPS '24*. Curran Associates Inc., 2024.

Meng, K., Bau, D., Andonian, A., and Belinkov, Y. Locating and editing factual associations in gpt, 2023.

Nguyen, T., Li, Y., Ojha, U., and Lee, Y. J. Visual instruction inversion: Image editing via visual prompting, 2023.

Peng, Z., Wang, W., Dong, L., Hao, Y., Huang, S., Ma, S., and Wei, F. Kosmos-2: Grounding multimodal large language models to the world. *arXiv preprint arXiv:2306.14824*, 2023.

Ren, X., Li, C., Wang, S., and Li, B. Practice of the conformer enhanced audio-visual hubert on mandarin and english. In *ICASSP 2023 - 2023 IEEE International Conference on Acoustics, Speech and Signal Processing (ICASSP)*, pp. 1–5, 2023.

Shi, Z., Wan, G., Wang, H., Li, R., Huang, Z., Zhao, W., Xiao, Y., Luo, X., Yang, C., Sun, Y., and Wang, W. Don't forget the enjoin: FocalloRA for instruction hierarchical alignment in large language models. In *The Thirty-ninth Annual Conference on Neural Information Processing Systems*, 2025.

Stolfo, A., Balachandran, V., Yousefi, S., Horvitz, E., and Nushi, B. Improving instruction-following in language models through activation steering. In *The Thirteenth International Conference on Learning Representations*, 2025.

Tamayo, D., Gonzalez-Agirre, A., Hernando, J., and Villegas, M. Mass-editing memory with attention in transformers: A cross-lingual exploration of knowledge. In *Findings of the Association for Computational Linguistics ACL 2024*, pp. 5831–5847. Association for Computational Linguistics, 2024.

Turner, A. M., Thiergart, L., Leech, G., Udell, D., Vazquez, J. J., Mini, U., and MacDiarmid, M. Steering language models with activation engineering, 2024.

Wang, P., Bai, S., Tan, S., Wang, S., Fan, Z., Bai, J., Chen, K., Liu, X., Wang, J., Ge, W., et al. Qwen2-vl: Enhancing vision-language model's perception of the world at any resolution. *arXiv preprint arXiv:2409.12191*, 2024.

Wu, X., Yao, W., Chen, J., Pan, X., Wang, X., Liu, N., and Yu, D. From language modeling to instruction following: Understanding the behavior shift in LLMs after instruction tuning. In Duh, K., Gomez, H., and Bethard, S. (eds.), *Proceedings of the 2024 Conference of the North American Chapter of the Association for Computational Linguistics: Human Language Technologies (Volume 1: Long Papers)*, pp. 2341–2369, Mexico City, Mexico, June 2024. Association for Computational Linguistics.

Xu, J., Guo, Z., He, J., Hu, H., He, T., Bai, S., Chen, K., Wang, J., Fan, Y., Dang, K., et al. Qwen2. 5-omni technical report. *arXiv preprint arXiv:2503.20215*, 2025.

Yang, Y., Nushi, B., Palangi, H., and Mirzasoleiman, B. Mitigating spurious correlations in multi-modal models during fine-tuning. In Krause, A., Brunskill, E., Cho,

K., Engelhardt, B., Sabato, S., and Scarlett, J. (eds.), *Proceedings of the 40th International Conference on Machine Learning*, volume 202 of *Proceedings of Machine Learning Research*, pp. 39365–39379. PMLR, 23–29 Jul 2023.

Ye, H., Yang, C.-H. H., Goel, A., Huang, W., Zhu, L., Su, Y., Lin, S., Cheng, A.-C., Wan, Z., Tian, J., et al. Omnidivinci: Enhancing architecture and data for omni-modal understanding llm. *arXiv preprint arXiv:2510.15870*, 2025.

Ye, W., Zheng, G., Ma, Y., Cao, X., Lai, B., Rehg, J. M., and Zhang, A. MM-spubench: Towards better understanding of spurious biases in multimodal LLMs. In *Workshop on Responsibly Building the Next Generation of Multimodal Foundational Models*, 2024.

Yuan, Y., Zhao, L., Zhang, K., Zheng, G., and Liu, Q. Do llms overcome shortcut learning? an evaluation of shortcut challenges in large language models, 2024.

Zhang, H., Wang, X., Li, C., Ao, X., and He, Q. Controlling large language models through concept activation vectors. *Proceedings of the AAAI Conference on Artificial Intelligence*, 39(24):25851–25859, Apr. 2025.

Zhang, J., Ma, X., Guo, S., Li, P., Xu, W., Tang, X., and Hong, Z. Amend to alignment: decoupled prompt tuning for mitigating spurious correlation in vision-language models. In *Proceedings of the 41st International Conference on Machine Learning*, ICML’24. JMLR.org, 2024a.

Zhang, N., Tian, B., Cheng, S., Liang, X., Hu, Y., Xue, K., Gou, Y., Chen, X., and Chen, H. Instructedit: Instruction-based knowledge editing for large language models. In Larson, K. (ed.), *Proceedings of the Thirty-Third International Joint Conference on Artificial Intelligence, IJCAI-24*, pp. 6633–6641. International Joint Conferences on Artificial Intelligence Organization, 8 2024b. Main Track.

Zhang, X., Yoon, J., Bansal, M., and Yao, H. Multimodal representation learning by alternating unimodal adaptation. In *Proceedings of the IEEE/CVF conference on computer vision and pattern recognition*, pp. 27456–27466, 2024c.

Zhu, H., Liu, Y., Fang, X., Lu, G., and Chen, B. Cause-effect driven optimization for robust medical visual question answering with language biases. In Kwok, J. (ed.), *Proceedings of the Thirty-Fourth International Joint Conference on Artificial Intelligence, IJCAI-25*, pp. 2512–2520. International Joint Conferences on Artificial Intelligence Organization, 8 2025.

Zou, A., Phan, L., Chen, S., Campbell, J., Guo, P., Ren, R., Pan, A., Yin, X., Mazeika, M., Dombrowski, A.-K., Goel, S., Li, N., Byun, M. J., Wang, Z., Mallen, A., Basart, S., Koyejo, S., Song, D., Fredrikson, M., Kolter, J. Z., and Hendrycks, D. Representation engineering: A top-down approach to ai transparency, 2025.

A. Technical Reference

Datasets All dataset links provided refer to the official sources released by the original authors or dataset maintainers, ensuring authenticity and traceability. We intentionally selected official resources to support reproducibility and transparency of the experimental setup. For MM-IMDb, we use a reconstructed subset of the dataset as a deliberate design choice to better isolate the effect of instruction-conditioned reliance, rather than to maximize task performance.

1. Tiny MM-IMDb: <https://www.kaggle.com/datasets/gabrieltardochi/tiny-mm-imdb>
2. CREMA-D: <https://gitlab.com/cs-cooper-lab/crema-d-mirror>
3. RAVDESS: <https://zenodo.org/records/1188976#.Xpaa3i-caAP>

Models We use Qwen2.5-VL-7B-Instruct(<https://huggingface.co/Qwen/Qwen2.5-VL-7B-Instruct>), Qwen2.5-VL-32B-Instruct(<https://huggingface.co/Qwen/Qwen2.5-VL-32B-Instruct>), and Gemma-3n-E4B-it(<https://huggingface.co/google/gemma-3n-E4B-it>) for the text-image modality setting, and Qwen2.5-Omni-7B(<https://huggingface.co/Qwen/Qwen2.5-Omni-7B>), AV-HuBERT(<https://huggingface.co/vumichien/AV-HuBERT>), and AudioCLIP(<https://github.com/AndreyGuzhov/AudioCLIP>) for the audio-video modality setting, with all models obtained exclusively from their official releases to ensure authenticity and reproducibility.

The Qwen2.5-VL family provides strong general-purpose vision-language capabilities, Gemma-3n-E4B-it serves as a lightweight instruction-tuned multimodal baseline. Also, Qwen2.5-Omni-7B supports unified multimodal understanding across audio, vision, and language, AV-HuBERT offers robust self-supervised audio-visual speech representations, and AudioCLIP enables aligned representation learning across audio, vision and text, collectively allowing us to evaluate instruction-conditioned reliance across diverse multimodal architectures and learning paradigms. A detailed description of the experimental protocols involving these models, as well as the corresponding results, is provided in Section 5.5.

B. Dataset-Intrinsic Feature Composition Analysis

We analyze the intrinsic composition of core and spurious features across datasets, independent of any model predictions. For each dataset, we aggregate annotated feature tags according to a hierarchical feature taxonomy and report their relative proportions by modality and feature group. Figure 7 shows the overall feature composition across all datasets, while Figures 8, 9, and 10 present the detailed breakdowns for MM-IMDb, CREMA-D, and RAVDESS, respectively.

Across all datasets, core and spurious features are not evenly distributed but instead exhibit pronounced skew toward one role within most feature groups. In particular, demographic- and background-related features consistently show a high proportion of spurious annotations, indicating that these cues are structurally well-suited for shortcut learning. In contrast, semantic, narrative, and expression-related features tend to be predominantly core-aligned.

We observe substantial dataset-specific differences in how these feature groups are distributed. MM-IMDb exhibits extreme visual dominance, with appearance-related features accounting for the largest share of annotations. This dataset also contains a higher overall proportion of spurious visual features compared to the other datasets, suggesting that visual shortcuts are especially accessible. By contrast, CREMA-D and RAVDESS display more balanced modality distributions, with emotion-relevant features such as static and dynamic expressions exhibiting high core ratios.

Cross-dataset comparisons further reveal modality-specific structure. The image-based MM-IMDb dataset is dominated by appearance-related features, whereas the video-based datasets (CREMA-D and RAVDESS) are dominated by static expression features. Background and identity-related cues (e.g., skin tone and language) are rare in CREMA-D and RAVDESS, consistent with their controlled recording environments, but appear more frequently in MM-IMDb.

These dataset-intrinsic statistics motivate our focus on instruction-conditioned reliance control. When spurious cues are concentrated within specific modalities or feature groups, shortcut learning becomes structurally advantageous unless reliance is explicitly regulated.

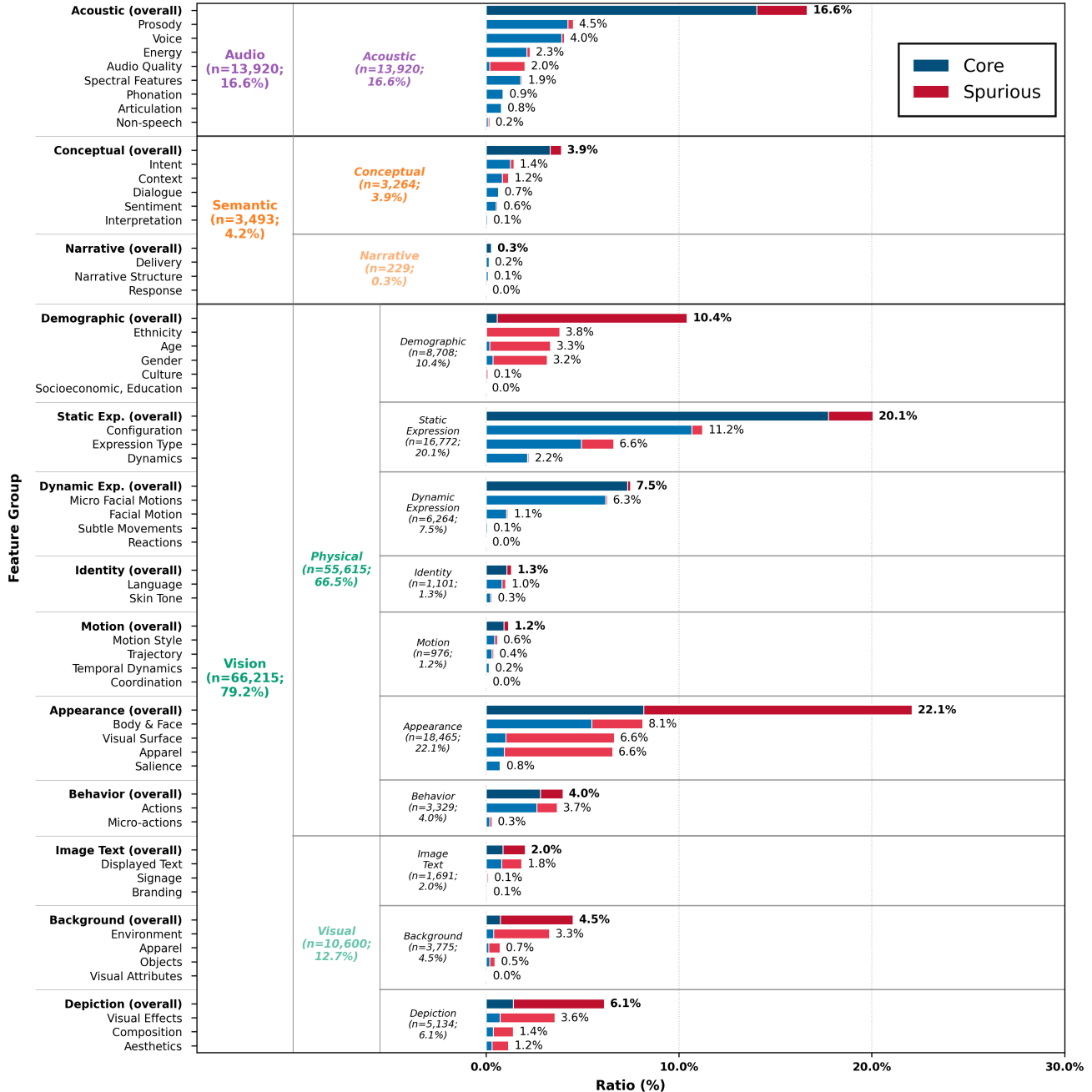


Figure 7. Aggregated core and spurious feature composition across all datasets. Visual appearance, background, and static expression features account for a large fraction of spurious annotations, whereas semantic and narrative features are predominantly core-aligned. This aggregation highlights recurring structural patterns that make shortcut learning advantageous in multimodal settings.

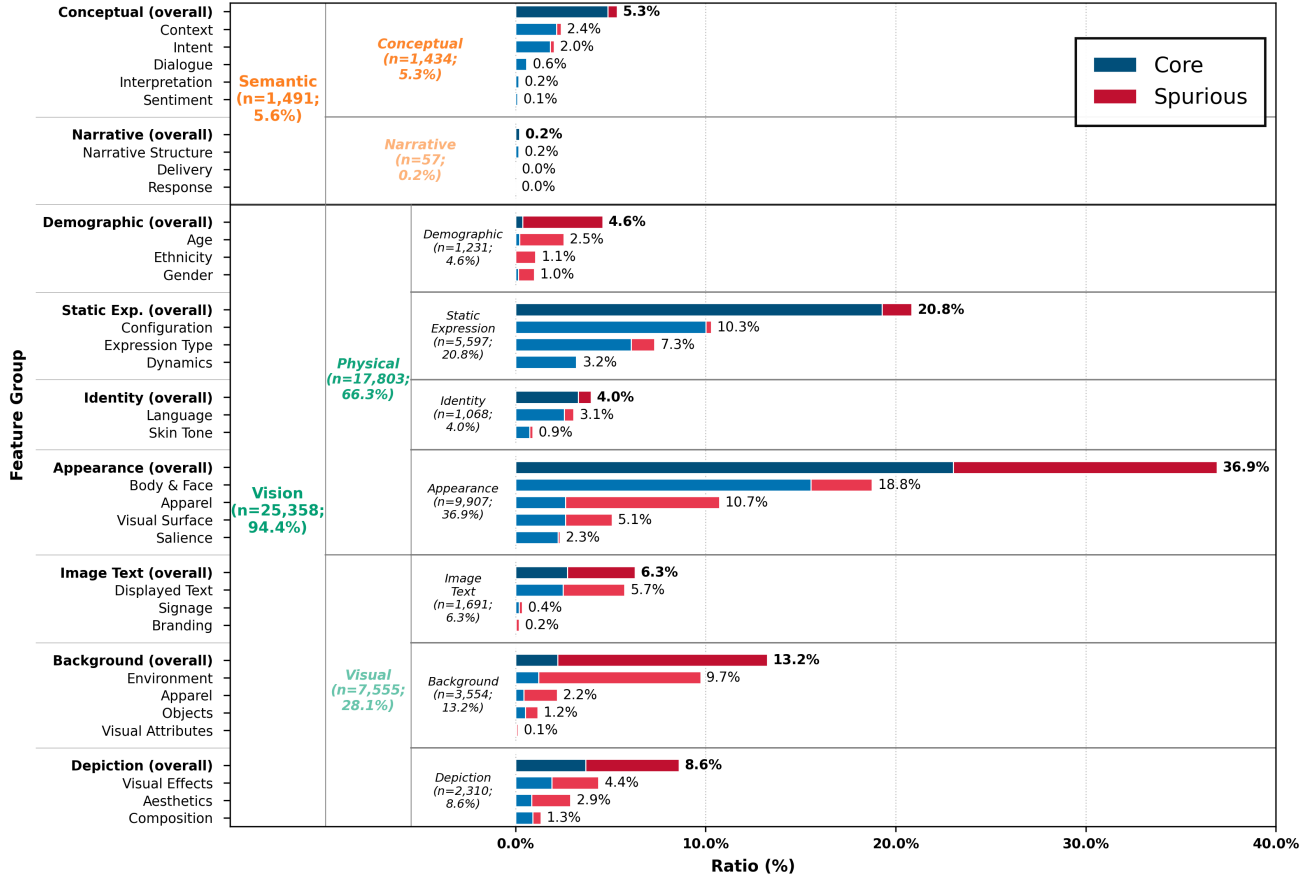


Figure 8. Dataset-intrinsic composition of core and spurious feature annotations for MM-IMDb. The dataset exhibits strong visual dominance, with appearance-related features accounting for a large share of annotations. Compared to the other datasets, MM-IMDb contains a higher proportion of spurious visual features, indicating favorable conditions for visual shortcut learning.

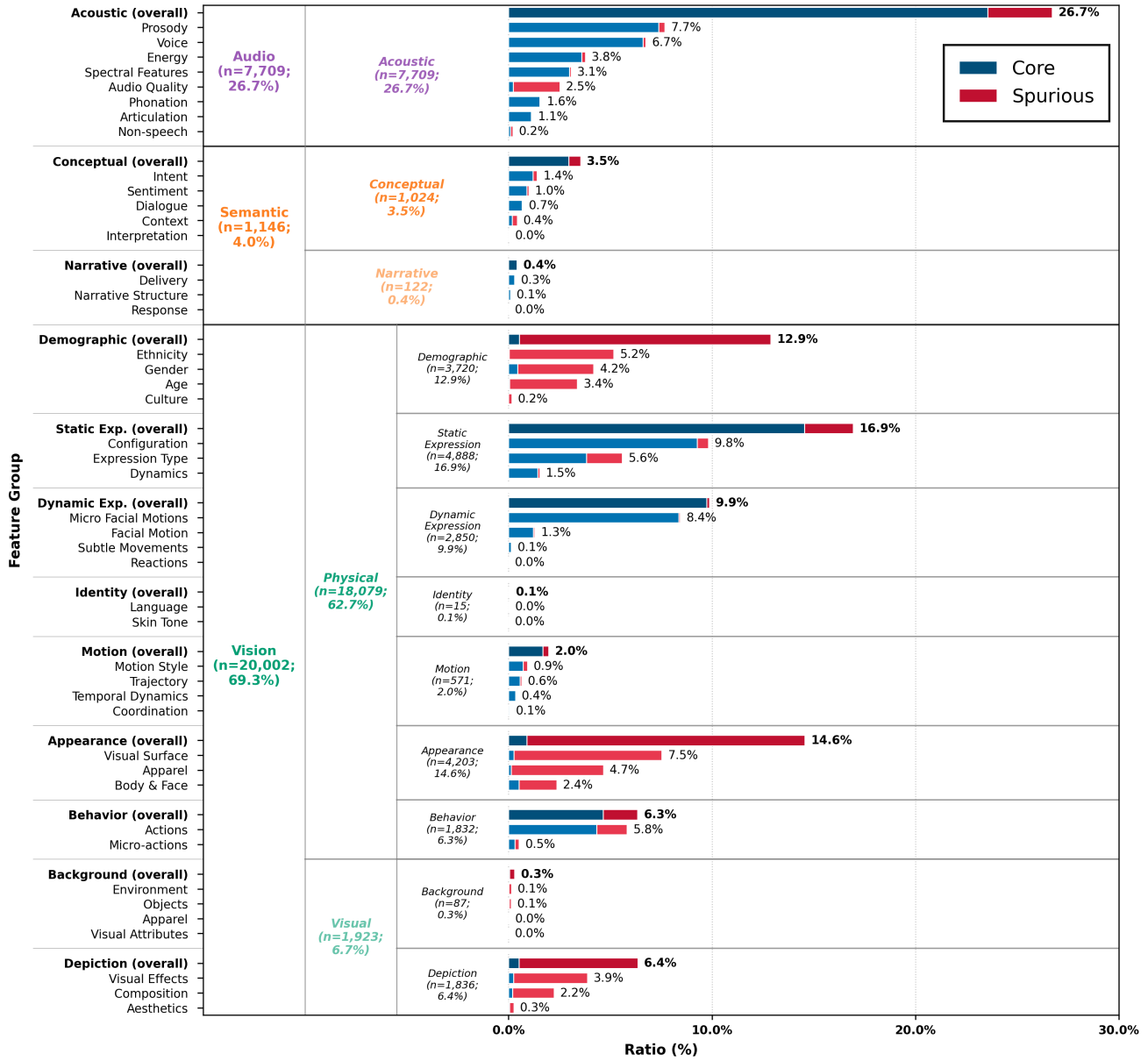


Figure 9. Dataset-intrinsic composition of core and spurious feature annotations for CREMA-D. Emotion-relevant expression features are predominantly core-aligned, while demographic cues contribute a non-negligible share of spurious annotations. Overall modality distributions and core-spurious patterns are similar to those observed in RAVDESS.

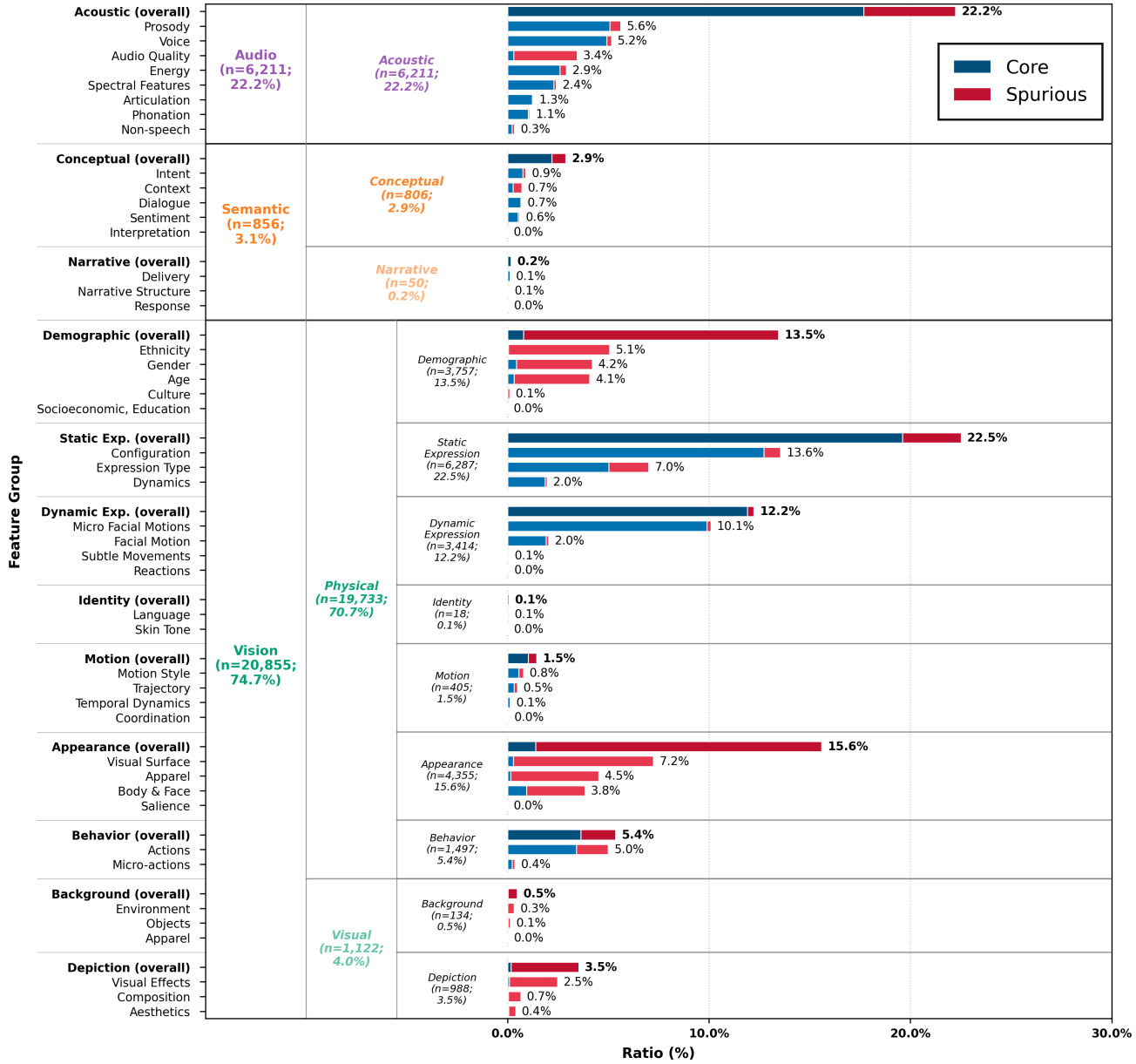


Figure 10. Dataset-intrinsic composition of core and spurious feature annotations for RAVDESS, organized by modality and feature group. Acoustic and expression-related features dominate the annotation space and are predominantly core-aligned, while demographic and background cues appear less frequently.

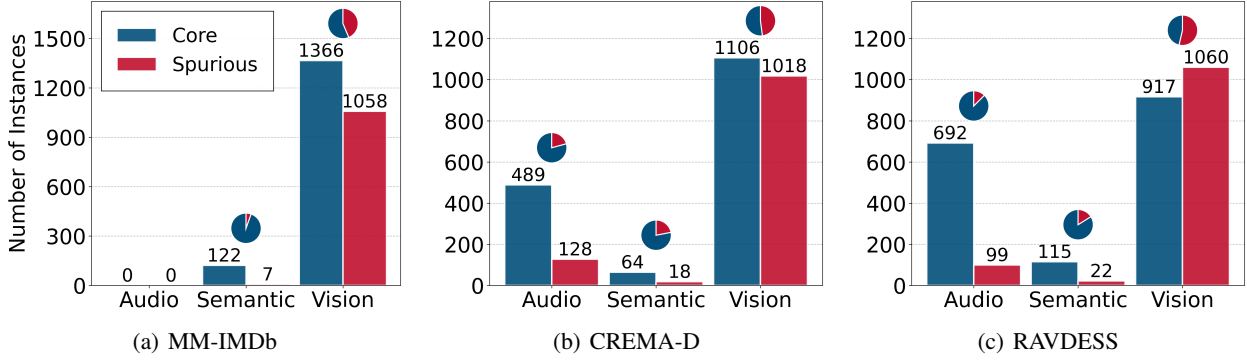


Figure 11. Modality-wise counts of annotated core and spurious features for MM-IMDb, CREMA-D, and RAVDESS. Bars indicate the total number of feature annotations per modality, while inset pies show the relative core-spurious composition within each modality. Vision accounts for the largest volume of annotations across datasets, highlighting its potential as a dominant source of shortcut cues.

C. Modality-Level Distribution of Core and Spurious Features

This section reports the absolute number of annotated core and spurious features by modality for each dataset, as shown in Figure 11. Unlike ratio-based analyses, this view highlights the raw volume of available cues within each modality, which determines the size of the shortcut search space prior to any model training. Across MM-IMDb, CREMA-D, and RAVDESS, vision consistently accounts for the largest number of feature annotations, encompassing both core and spurious cues. This dominance indicates that visual modalities provide a particularly rich and diverse set of signals, making shortcut learning structurally more accessible than in audio or semantic modalities. While the overall prominence of vision is consistent, the relative balance between core and spurious features within vision varies across datasets. MM-IMDb and CREMA-D exhibit a higher proportion of core-aligned visual features, whereas RAVDESS shows a comparatively larger share of spurious visual annotations. In contrast, audio and semantic modalities are consistently core-dominant across all datasets, suggesting that task-relevant information is more uniformly represented in these modalities. Differences in the semantic modality further reflect dataset characteristics. In MM-IMDb, semantic features are predominantly core-aligned, consistent with the relevance of plot descriptions to genre labels. By contrast, in CREMA-D and RAVDESS, semantic annotations show a higher spurious proportion, reflecting the weaker association between spoken content and emotion labels. Overall, this modality-level analysis complements the feature group breakdown presented in Appendix B. Together, these analyses characterize where shortcut-prone cues are concentrated in the data and motivate the need for explicit, instruction-conditioned regulation of modality reliance.

D. Label–Feature Associations and Core–Spurious Misalignment

This appendix examines which feature groups are most strongly associated with target labels prior to any model intervention. For each dataset, we compute the mutual information (MI) between feature group annotations and ground-truth labels, and rank feature groups by their MI scores. For each of the top-ranked feature groups, we additionally report whether its empirical usage is dominated by core or spurious annotations. Figure 6 shows the MI between feature groups and labels across all datasets, ranked by association strength. Across datasets, a substantial fraction of the feature groups most strongly associated with labels are spurious-dominant. Among the top-20 feature groups ranked by MI, several exhibit higher spurious usage than core usage, demonstrating that strong statistical association with labels does not imply task relevance. This finding highlights a key limitation of correlation-driven learning: features that are highly predictive may reflect dataset-specific shortcuts rather than causal or semantic signals. Dataset-specific analyses further illustrate this phenomenon. In MM-IMDb, visually salient appearance and environment-related features exhibit higher MI with genre labels than several expression- or configuration-related features that are predominantly core. (Figure 12) In CREMA-D, low-level visual attributes such as visual surface and visual effects show stronger label association than micro facial motions, despite the latter being more semantically aligned with emotional expression. (Figure 13) In RAVDESS, the MI values of core-dominant expression features and spurious-dominant visual surface features are comparable, indicating that spurious cues can be as predictive as task-relevant ones even in controlled datasets. (Figure 14) Overall, this analysis demonstrates that mutual information alone is insufficient to distinguish core from spurious features. The coexistence of high label association and spurious dominance motivates the need for explicit mechanisms that regulate internal feature reliance beyond correlation-based optimization.

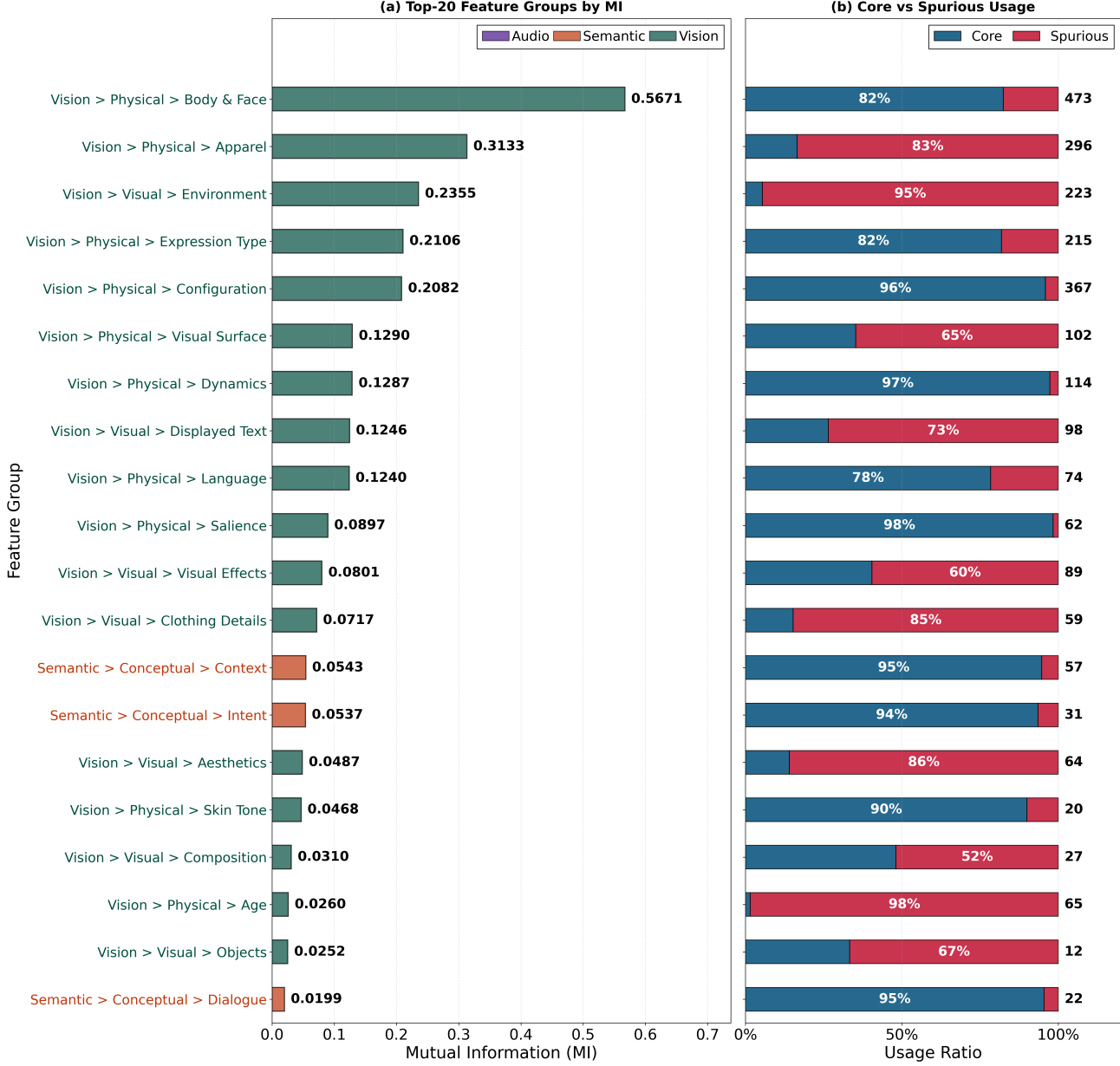


Figure 12. Top-20 feature groups ranked by mutual information (MI) with target labels for the MM-IMDb dataset. Panel (a) shows MI values by feature group, and panel (b) reports the corresponding core versus spurious usage ratios. Highly predictive feature groups are not necessarily core-dominant, revealing dataset-specific shortcut structures.

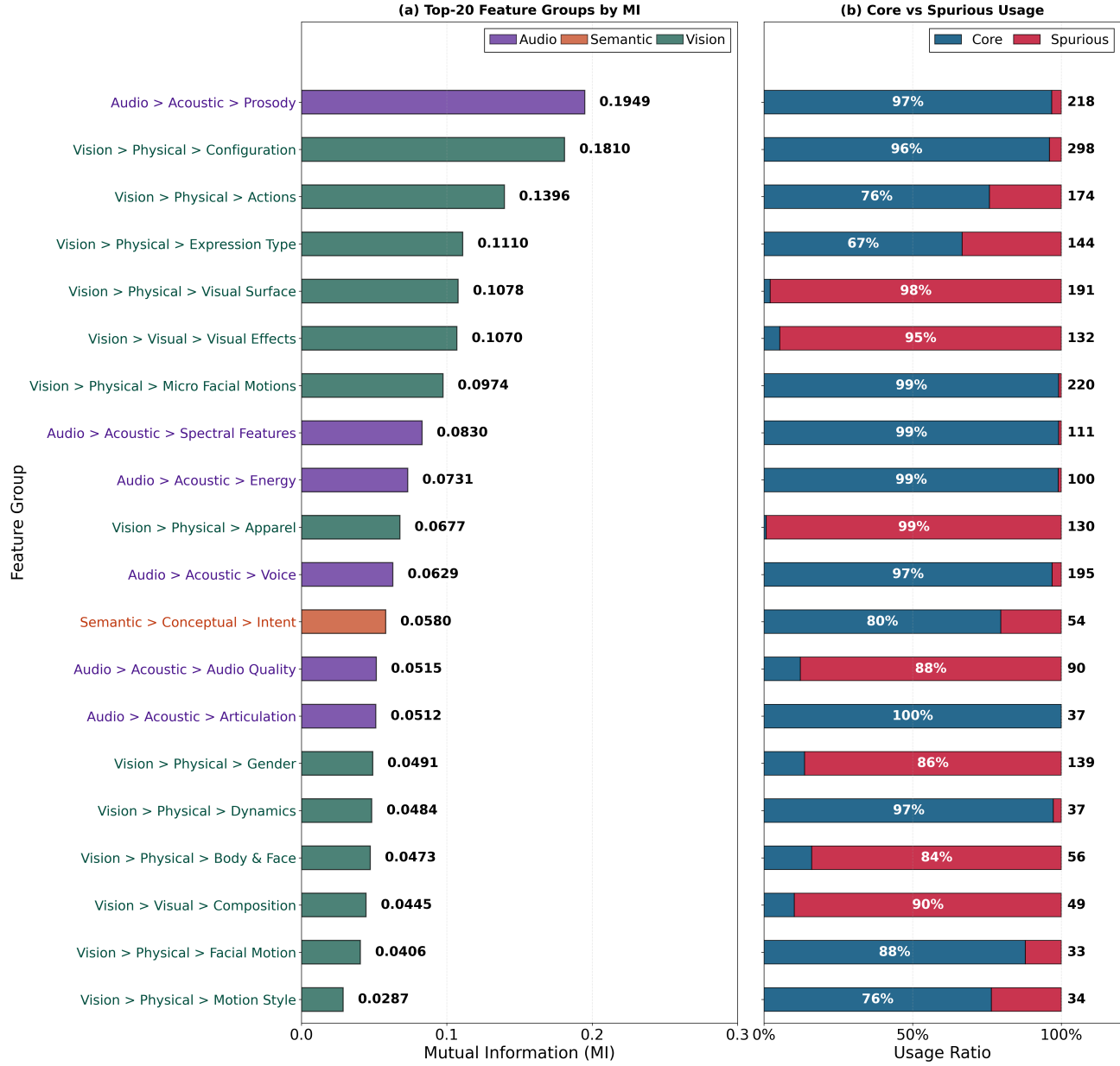


Figure 13. Top-20 feature groups ranked by mutual information (MI) with target labels for the CREMA-D dataset. Panel (a) shows MI values by feature group, and panel (b) reports the corresponding core versus spurious usage ratios. Highly predictive feature groups are not necessarily core-dominant, revealing dataset-specific shortcut structures.

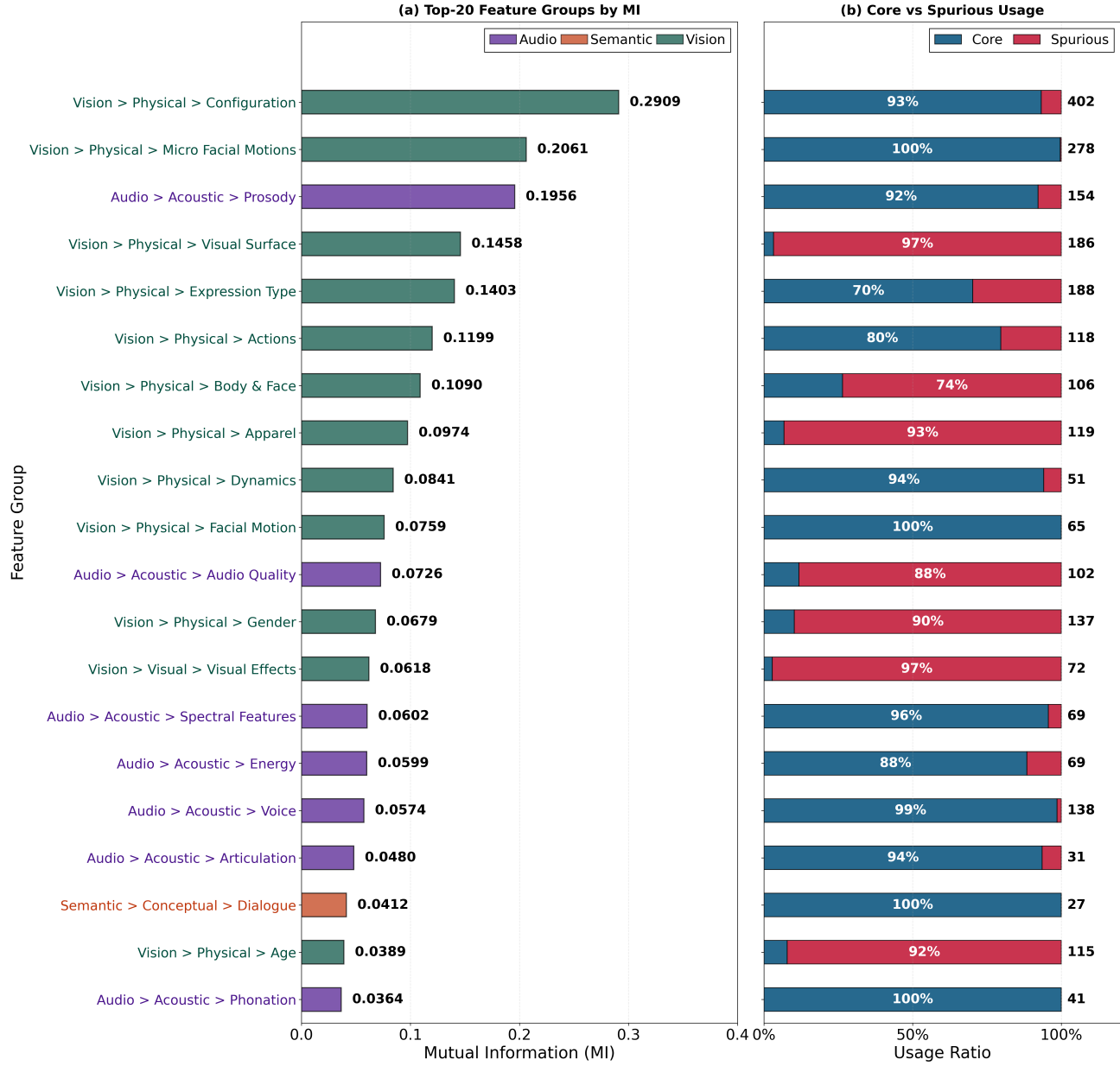


Figure 14. Top-20 feature groups ranked by mutual information (MI) with target labels for the RAVDESS dataset. Panel (a) shows MI values by feature group, and panel (b) reports the corresponding core versus spurious usage ratios. Highly predictive feature groups are not necessarily core-dominant, revealing dataset-specific shortcut structures.

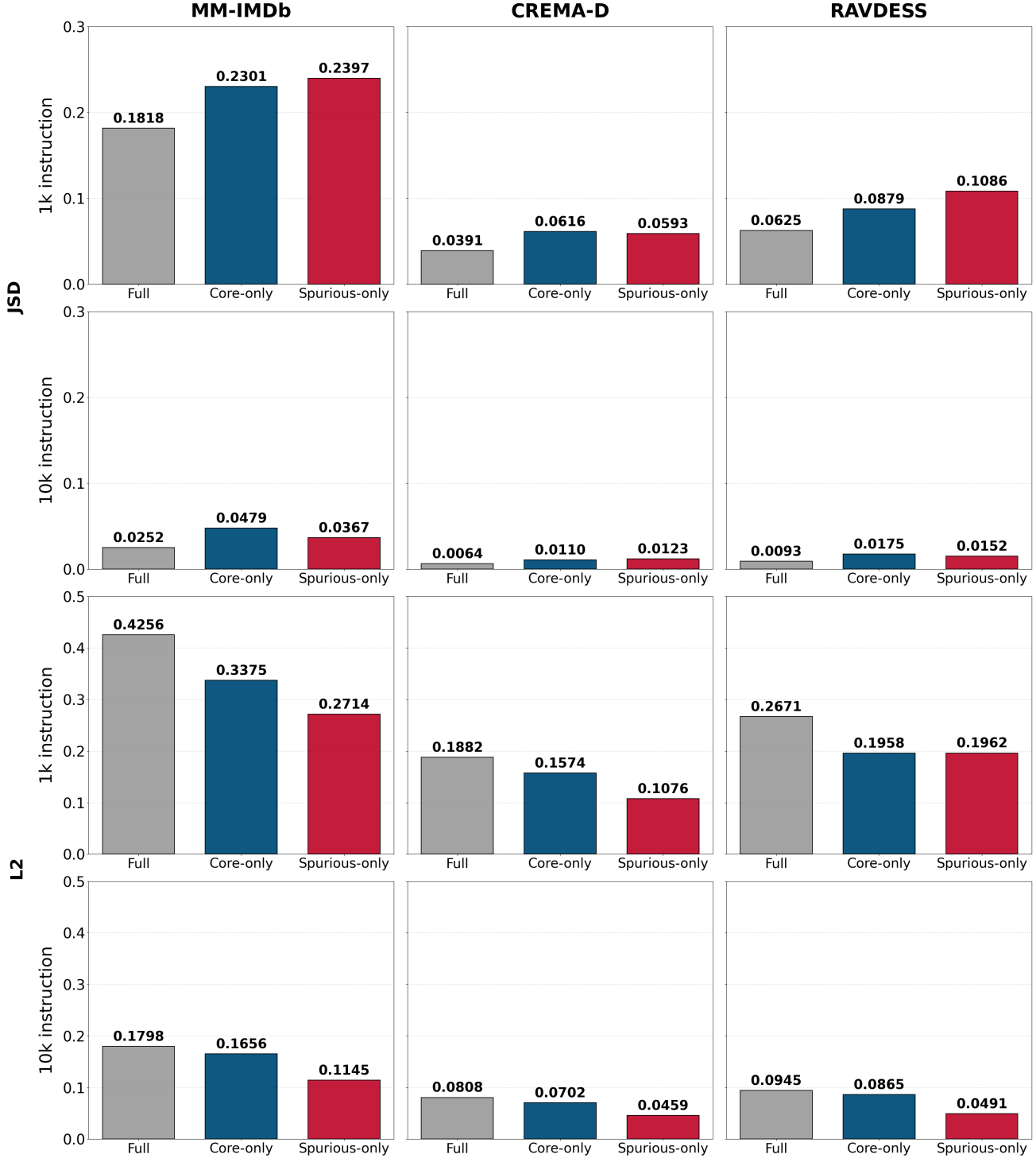


Figure 15. Label separability under different feature availability conditions. We measure Jensen-Shannon divergence (top) and ℓ_2 distance (bottom) between label-wise average feature representations under three settings: *Full* (all features), *Core-only* (spurious features removed), and *Spurious-only* (core features removed). Results are reported for 1k and 10k instruction variations across MM-IMDb, CREMA-D, and RAVDESS. Label separability differs only marginally between core-only and spurious-only conditions, indicating that spurious features alone can preserve substantial label structure.

E. Label Separability Under Core and Spurious Feature Conditions

This appendix analyzes how well target labels are separable under different feature availability conditions, as shown in Figure 15. Specifically, we compare label separability when using all available features (*Full*), only core features (*Core-only*), and only spurious features (*Spurious-only*). For each instruction, we construct a feature group occurrence vector by counting the feature groups activated under that instruction. We then compute label-wise average feature vectors and measure inter-label separability using two complementary metrics: Jensen-Shannon divergence (JSD), which captures distributional distinguishability, and ℓ_2 distance, which reflects geometric separation in feature space. We report results for 1k and 10k instruction variations to assess the effect of instruction diversity. Across datasets and instruction scales, JSD-based separability differs only marginally between core-only and spurious-only conditions. In several cases, particularly for MM-IMDb and RAVDESS under 1k instructions, spurious-only features yield equal or higher label separability than core-only features. This indicates that spurious features alone can support non-trivial label discrimination.

As the number of instructions increases to 10k, overall JSD values decrease across all conditions, suggesting that increased instruction diversity dilutes label-specific feature concentration. Notably, this degradation affects core-only and spurious-only conditions similarly, implying that neither feature subset uniquely preserves label separability at scale. The ℓ_2 distance analysis exhibits a consistent ordering across all datasets and instruction scales, with *Full* > *Core-only* > *Spurious-only*. However, the magnitude of these differences is modest, and spurious-only representations remain comparably separable from a geometric perspective.

Together, these results show that label separability alone does not reliably distinguish core from spurious features. Even when restricted to spurious features, the induced feature representations retain substantial label structure, explaining why correlation-driven learning can preferentially exploit spurious cues in practice.

F. Dataset-Specific Robustness to Spurious Feature Interventions

This appendix provides dataset-specific robustness analyses under spurious feature interventions, as shown in Figure 16. For each dataset, all baseline methods are evaluated on the appropriate backbone: Qwen2.5-VL for MM-IMDb and Qwen2.5-Omni for CREMA-D and RAVDESS. We report decision stability under spurious feature removal and performance degradation under progressive spurious suppression. While absolute robustness varies across datasets due to differences in spurious structure, all datasets exhibit consistent qualitative trends: FiLoRA preserves higher decision stability and degrades more gracefully than full fine-tuning, LoRA, and prompt-only baselines.

G. Construction of Spurious Proxy Labels

To enable controlled analysis of feature reliance, we construct spurious proxy labels that approximate predictions made when the model relies primarily on a restricted subset of input features. These proxy labels are used exclusively as a training-time intervention and are never used as evaluation targets. For each dataset, we specify feature subsets that are known to be predictive yet semantically incidental to the task, and we intend the proxy labels to reflect reliance on these cues.

In MM-IMDb, proxy labels are derived to emphasize visual appearance attributes of movie posters, such as color palettes, typography, and layout cues, while de-emphasizing semantic information conveyed by plot text. In CREMA-D and RAVDESS, proxy labels are constructed to emphasize low-level acoustic or surface-level visual cues, such as pitch statistics, energy contours, or coarse visual attributes, while discouraging reliance on features directly encoding emotional semantics.

Proxy labels are generated offline using a frozen large vision–language model (LVLM), prompted to make predictions based only on the specified restricted cues. Because such models may imperfectly follow focus–ignore instructions, we treat the resulting proxy labels as spur-leaning supervision signals rather than pure spurious ground truth. To mitigate semantic leakage, we apply input-level restrictions appropriate to each modality and report diagnostic analyses that quantify proxy–core label alignment and potential leakage effects.

Both the original task labels and the proxy labels lie in the same label space, and no new prediction objectives are introduced. The proxy labels serve solely to induce controlled reliance on spurious cues during training, enabling us to study how instruction-conditioned gating modulates internal feature usage under fixed task semantics. At evaluation time, all models are assessed exclusively with respect to the original task labels.

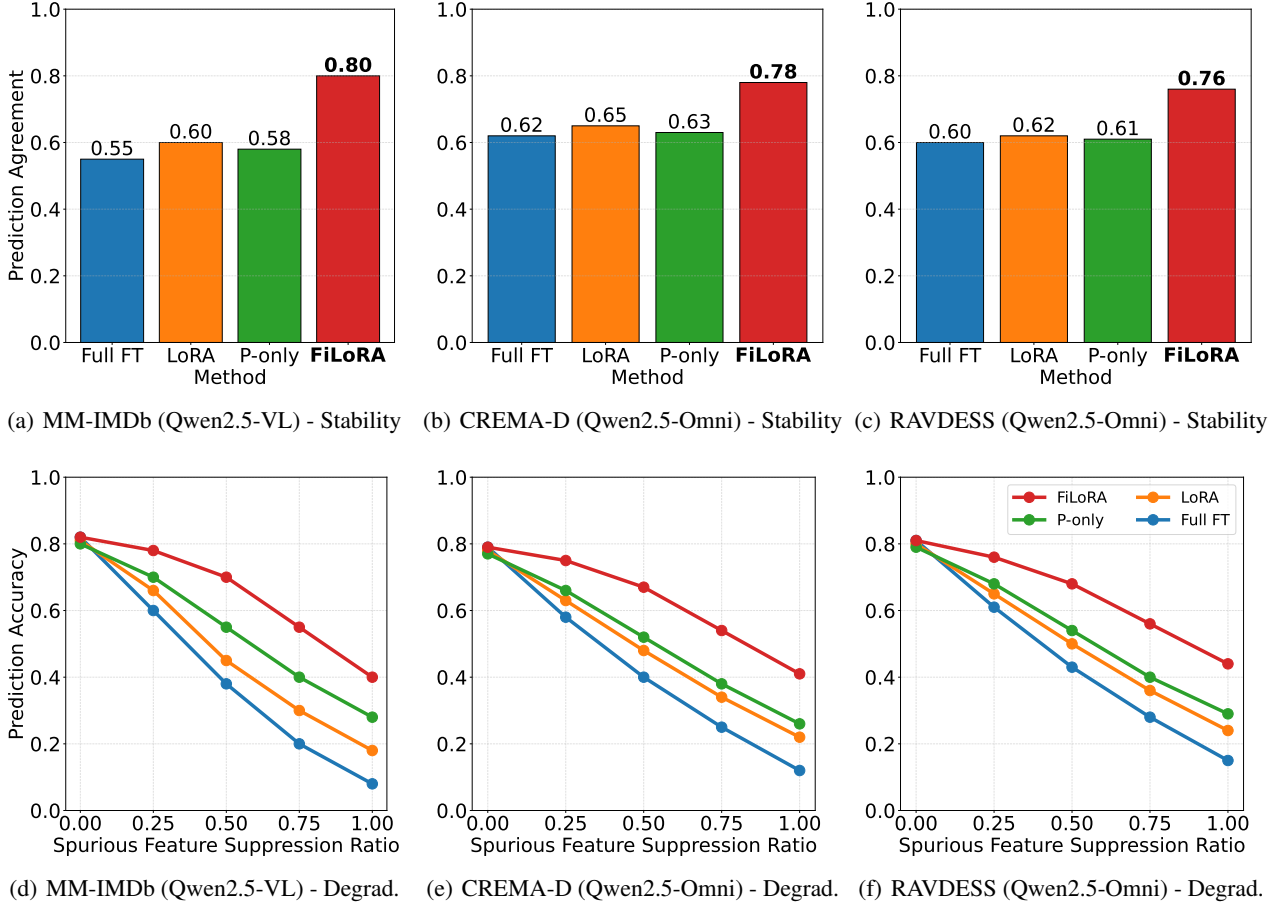


Figure 16. Dataset-specific decision stability under spurious feature removal (top, abbreviated as Stability) and performance degradation under increasing spurious feature suppression (bottom, abbreviated as Degrad.). For decision stability, prediction agreement is measured before and after removing spurious features. All baselines are evaluated on dataset-appropriate backbones. Across datasets, FiLoRA consistently preserves higher stability than full fine-tuning, LoRA, and P-only (prompt-only) baselines. For performance degradation, accuracy is reported as a function of spurious feature suppression ratio. Although degradation rates differ across datasets, FiLoRA consistently exhibits more gradual performance decline than baseline methods.

H. FiLoRA Training Procedure

This appendix provides a step-by-step description of the FiLoRA training procedure, complementing the methodological formulation presented in Section 3. Algorithm 1 summarizes how instruction-conditioned gating, grouped LoRA adaptation, and supervision routing are integrated during training. Each training sample consists of multimodal input x_i , a natural language instruction I_i , the original task label y_i , a spurious proxy label $y_i^{(s)}$, and an experimental condition c_i . The base multimodal model parameters remain frozen throughout training, and only grouped LoRA parameters and the instruction encoder are updated. At each training step, instructions are encoded into continuous control representations, which parameterize the instruction-conditioned gating function. These gates softly modulate the contribution of group-specific LoRA updates, enabling sample-wise and instruction-dependent control over internal computation paths. The supervision signal is selected according to the experimental condition, but the condition itself is never provided to the model. As a result, any learned shift in feature reliance must emerge from the interaction between instruction-conditioned gating and loss optimization, rather than from explicit conditioning on task identity. A weak gate regularization term is optionally applied to stabilize instruction-conditioned reliance patterns and prevent degenerate gate behavior. This regularization acts only as a soft inductive bias and does not impose hard constraints on gate activations. All predictions are evaluated exclusively with respect to the original task labels, ensuring that the learning setup remains a single-task formulation. Algorithm 1 is included to facilitate reproducibility and to clarify the end-to-end training flow of FiLoRA.

Algorithm 1 FiLoRA Training with Instruction-Conditioned Gating

Input: Training dataset $\{(x_i, I_i, y_i, y_i^{(s)}, c_i)\}_{i=1}^N$,
 Pretrained multimodal model f_θ (frozen),
 Grouped LoRA parameters $\{\Delta W_g\}_{g \in \mathcal{G}}$,
 Instruction encoder h_ϕ ,
 Gate regularization weight λ
Output: Trained grouped LoRA parameters and instruction encoder

for each training step **do**

- Sample minibatch $\mathcal{B} \subset \{1, \dots, N\}$
- for** each sample $i \in \mathcal{B}$ **do**

 - Encode instruction: $\mathbf{z}_i \leftarrow h_\phi(I_i)$
 - Compute gate vector: $\mathbf{g}_i \leftarrow \sigma(\mathbf{z}_i)$
 - Apply instruction-conditioned adaptation:
 $W' \leftarrow W + \sum_{g \in \mathcal{G}} g_{i,g} \Delta W_g$
 - Select supervision signal:

$$y_i^{\text{target}} = \begin{cases} y_i, & \text{if } c_i \text{ emphasizes core features,} \\ y_i^{(s)}, & \text{if } c_i \text{ emphasizes spurious features} \end{cases}$$
 - Compute classification loss:

$$\mathcal{L}_{\text{cls}}^{(i)} = \text{CE}(f(x_i, I_i), y_i^{\text{target}})$$
 - Compute gate regularization:

$$\mathcal{L}_{\text{gate}}^{(i)} = \sum_{g \in \mathcal{G}} \alpha_g^{(i)} g_{i,g}$$

- end**
- Update parameters by minimizing:

$$\sum_{i \in \mathcal{B}} (\mathcal{L}_{\text{cls}}^{(i)} + \lambda \mathcal{L}_{\text{gate}}^{(i)})$$

end

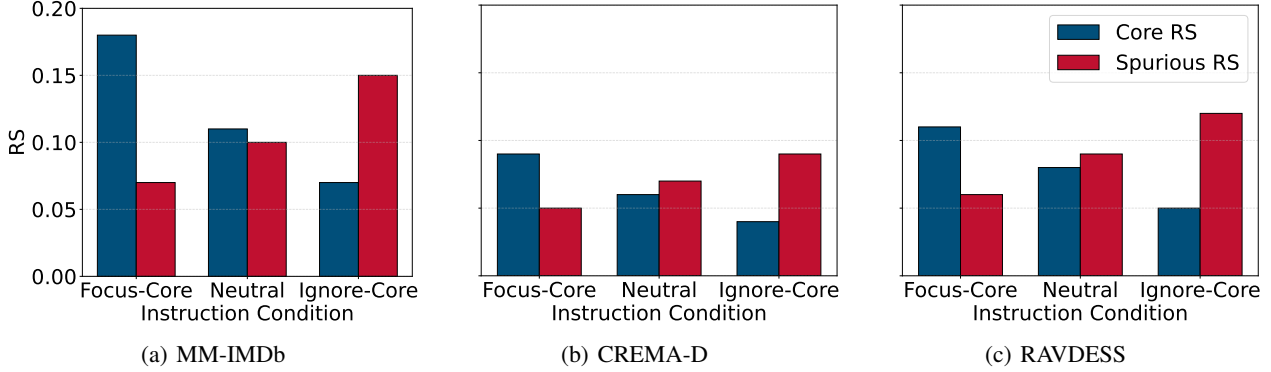


Figure 17. Dataset-wise prediction sensitivity to instruction-conditioned gate perturbations across MM-IMDb, CREMA-D, and RAVDESS. Focus-core instructions increase sensitivity to core-related features, while ignore-core instructions shift sensitivity toward spurious features.

I. Dataset-wise Reliance Sensitivity under Instruction-Conditioned Gating

Figure 17 shows that instruction-conditioned gating consistently redistributes prediction sensitivity between core and spurious features across datasets, providing direct evidence that reliance modulation produces functional changes in model behavior. The qualitative pattern mirrors the aggregate results in the main text, indicating that instruction-conditioned reliance modulation generalizes across modalities and dataset structures.

J. Instruction Dataset used for FiLoRA

Table 4 shows the models used for generating instructions and the total number of instructions created for each dataset. We employed multimodal models to generate focus-ignore instructions by taking actual data samples as input. Specifically, we used Qwen2.5-VL-7B-Instruct for the vision-language dataset (MM-IMDb) and Qwen2.5-Omni-7B for the audio-visual datasets (CREMA-D and RAVDESS). When training FiLoRA, 1,000 instructions were used for each dataset.

Dataset	Model	Total number of instructions
MM-IMDb	Qwen2.5-VL-7B-Instruct	1,000
CREMA-D	Qwen2.5-Omni-7B	1,000
RAVDESS	Qwen2.5-Omni-7B	1,000

Table 4. The number of instructions for each dataset. We used the Qwen2.5-VL for MM-IMDb and Qwen2.5-Omni for CREMA-D and RAVDESS. Instructions were generated by multimodal models using actual data samples as input to create focus-ignore instructions.

Dataset	Core RS	Spurious RS	Core / Spurious ratio
MM-IMDb	0.11	0.16	0.69
CREMA-D	0.14	0.10	1.40
RAVDESS	0.13	0.12	1.08

Table 5. Average reliance sensitivity (RS) under neutral instructions. Values reflect dataset-specific reliance balance between core and spurious features.

K. Dataset Selection Criteria

We select datasets according to three principled criteria that are necessary to support causal analysis of instruction-conditioned controllability. First, datasets must exhibit identifiable deterministic feature groups, such that low-level observable cues(e.g., acoustic traits and visual attributes) can be reliably mapped to higher-level modality or feature groups. This property ensures causally tracing the instruction-reliance pathway and also improves experimental reproducibility. Second, datasets should support diverse feature groups, enabling systematic and programmatic expansion of instruction templates. This allows us to generate large families of semantically equivalent instructions while reducing sensitivity to specific wording choices. Unlike feature removal or corruption-based analysis, FiLoRA enables continuous, instruction-conditioned modulation of internal reliance without altering the input distribution. Third, we require tasks with a fixed label space and stable objective, ensuring that variations across instruction conditions reflect changes in internal reliance rather than shifts in task semantics. In summary, datasets are chosen for (1) deterministic feature groups enabling causal traceability and reproducibility, and (2) compatibility with programmatic instruction expansion. We therefore focus on datasets where feature groups can be reasonably distinguished, as this supports clearer analysis and interpretation of instruction-conditioned changes in internal reliance.

L. Implementation Details

All experiments were conducted on a single **NVIDIA H100 NVL GPU (94GB memory)** using mixed-precision training (bf16). We used the AdamW optimizer with a batch size of 16, learning rates of 2×10^{-4} for grouped LoRA parameters and 1×10^{-4} for the instruction encoder, and a weight decay of 1×10^{-2} . Gradient norms were clipped at 1.0. Backbone multimodal models were kept frozen throughout training.

FiLoRA employs grouped LoRA adaptation with rank 8 and scaling factor 16. Instruction-conditioned gating produces a per-instruction gate vector with dimension equal to the number of LoRA groups. The instruction encoder is implemented as a lightweight 2-layer Transformer with hidden dimension 512 and GELU activations. A weak gate regularization term is applied to prevent degenerate gating behavior.

Training required approximately 2–3 hours per run depending on the dataset and backbone, resulting in a total compute budget of roughly **120 GPU-hours** on H100 NVL GPUs. All random seeds were fixed to ensure reproducibility.